M 2022

U.PORTO
FEUP FACULDADE DE ENGENHARIA
UNIVERSIDADE DO PORTO

DEVELOPMENT OF EMULSION PRODUCTS FROM NATURAL RAW MATERIALS

MARIANA MARQUES MAIO PEREIRA
MASTER THESIS IN CHEMICAL ENGINEERING
PRESENTED TO THE FACULTY OF ENGINEERING
OF THE UNIVERSITY OF PORTO

Master in Chemical Engineering

Development of emulsion products from natural raw materials

Master Dissertation

of

Mariana Marques Maio Pereira

Developed within the Course of Dissertation

held in

LSRE-LCM – Laboratory of Separation and Reaction Engineering – Laboratory of Catalysis and Materials

LEPABE – Laboratory for Process Engineering, Environment, Biotechnology and Energy

ALiCE – Associate Laboratory in Chemical Engineering

UCM – Universidad Complutense de Madrid

Supervisor at FEUP: **Margarida Brito**

Joint supervisor at FEUP: **Yaidelin A. Manrique**

Coordinator at UCM: **Ángeles Blanco**

U.PORTO
FEUP FACULDADE DE ENGENHARIA UNIVERSIDADE DO PORTO

DEPARTAMENTO DE ENGENHARIA QUÍMICA

July 2022

Acknowledgment

To my supervisors at FEUP, Doctor Margarida Brito and Doctor Yaidelin Manrique, for their constant involvement, knowledge sharing, encouragement, and support in the execution of this dissertation. I thank them for their confidence in assigning me this project that contributed significantly to my personal and professional growth.

To my supervisor at UCM, Professor Angeles Blanco, for giving me the exceptional opportunity of developing part of this project at UCM with the Advanced Water Treatments research group. I thank her for the excellent welcome, availability, and readiness to answer all my questions during these months of work.

To Doctor Ricardo Santos for the opportunity to develop this project and for all the supervision and suggestions.

To Professor Madalena Dias for the possibility to integrate the LSRE-LCM - Laboratory of Separation and Reaction Engineering - Laboratory of Catalysis and Materials and for the suggestions made.

To PhD student Jose Sanchez-Salvador for the excellent reception and integration at UCM, as well as all the support during the execution of this project and the readiness to help me whenever I needed.

To M.Eng. Ana Rita Fernandes who helped me obtain results that I needed for this project.

To my family, especially my parents and brother, who have always been present and supported me in all my achievements. I thank them for providing me with all the conditions for my personal and professional growth and motivating me to pursue all my ambitions.

To Gonçalo, who encouraged me every day and kept me organized with my daily planners and post-it notes. I thank him for always being present and knowing how to help me during the most challenging moments when things did not go as planned.

To all my friends for their indispensable daily motivation throughout these months. For all the laughs and the late night "francesinhas" dinners finishing the last details of this dissertation. For the Camélia surprises. For all the sing-alongs in the car. Without you, it wouldn’t make sense.

This work was financially supported by: LA/P/0045/2020 (ALiCE), UIDB/50020/2020 and UIDP/50020/2020 (LSRE-LCM) and UIDB/00511/2020 and UIDP/00511/2020 (LEPABE) funded by national funds through FCT/MCTES (PISSAC); project S4Hort_Soil&Food (NORTE-01-0145-FEDER-000074), supported by Programa Operacional Regional do Norte (NORTE 2020), through Portugal 2020 and Fundo Europeu de Desenvolvimento Regional (FEDER); Project RETOPROSOST 2-CM-P2018/EMT4459 Sustainable Production in Madrid Community.

Abstract

Currently, agricultural residues are mostly being burnt or tossed away as waste, which may cause several environmental problems. These residues are in general high in cellulosic content, which has raised the interest in their valorisation. An example is the isolation of cellulose nanofibres (CNF) and microfibres (CMF) that can be used in many applications, including as emulsifiers in Pickering emulsions.

Pickering emulsions use solid particles to stabilize the oil/water (O/W) interface, granting higher stability against coalescence than emulsions stabilized by surfactants. They are a promising lower-calorie alternative to the unhealthy fats used in the food industry. Moreover, the application of Pickering emulsifiers in foodstuffs is safer and healthier than surfactants since they can be produced from natural sources. The objective of this work was to study the best formulation for the stability of emulsions using cellulose micro/nanofibres obtained from grocery waste.

Two cellulosic raw-materials, leek and lettuce, provided by a greengrocer's shop as food waste, have been studied. CNF/CMF were obtained without any chemical pre-treatment. To facilitate fibrillation, both raw materials were subjected to different treatment combinations (drying, milling, disintegration with water in a blender) to obtain chemically unmodified cellulose fibres. Fibrillation was then carried out by a mechanical treatment in a high-pressure homogenizer (HPH) at different conditions. A full morphological characterization of the samples was made to monitor the fibrillation process.

The fibres were then used to stabilize sunflower oil-in-water Pickering emulsions. Results showed that drying, milling, and disintegration were the best combination of pre-treatments in terms of fibres' diameter reduction. With these pre-treatments, CMF was produced after homogenization. Using the pulps containing chemically unmodified CMF, Pickering emulsions were prepared at different O/W ratios (20/80-70/30 wt.%) and pulps' solid content in the aqueous phase (PSC) (1.0-4.8 wt.%). The oil was dispersed into the aqueous phase using a rotor-stator homogenizer to obtain a homogeneous emulsion phase. The best stability results were obtained when the pre-treated leek was homogenized at high consistency with 6 passes of HPH at 600 bar. On the other hand, the pre-treated lettuce was centrifugated with no additional HPH.

After 48 h, the visual inspection of emulsions showed that there was at least one formulation for each O/W ratio with an emulsifying index (EI) higher than 92 wt.%, demonstrating the feasibility of using leek and lettuce residues to produce Pickering emulsions. In addition, results also indicated that the increase in PSC resulted in a higher emulsion phase.

This work shows for the first-time the production of stable Pickering emulsions containing cellulose from leek and lettuce pulps. These results may contribute to develop circular economy processes, by using biobased products, and open new market niches and business models.

Keywords: Pickering emulsions; agricultural waste; cellulose; micro cellulose fibres; food application

Resumo

Atualmente, os resíduos agrícolas estão maioritariamente a ser queimados ou descartados como lixo, o que pode causar vários problemas ambientais. Estes resíduos são compostos, em geral, por um elevado conteúdo de celulose, o que tem suscitado interesse pela sua valorização. Um exemplo é o isolamento de nano (CNF) e microfibras de celulose (CMF) que podem ser utilizadas como emulsificantes em emulsões Pickering.

As emulsões Pickering utilizam partículas sólidas para estabilizar a interface óleo/água (O/W), conferindo maior estabilidade contra a coalescência do que as estabilizadas por tensioativos tradicionais. São uma alternativa promissora de menor teor calórico às gorduras insalubres utilizadas na indústria alimentar. Além disso, a aplicação de emulsificantes Pickering é mais segura e saudável, uma vez que podem ser de origem natural. O objetivo deste trabalho foi o estudo da melhor formulação para a estabilidade das emulsões, utilizando micro/nanofibras de celulose obtidas a partir de desperdício alimentar.

Estudaram-se duas matérias-primas celulósicas, alho francês e alface, fornecidas por uma mercearia como desperdício alimentar. Foram obtidos CMF/CNF sem qualquer tratamento químico. Para facilitar a fibrilação, ambas as matérias-primas foram submetidas a diferentes pré-tratamentos mecânicos (secagem, moagem, desintegração com água numa liquidificadora) para obter fibras de celulose quimicamente inalteradas. Seguiu-se a fibrilação por tratamento mecânico num homogeneizador a alta pressão (HPH) a diferentes condições, que foi monitorizada por uma caracterização morfológica das amostras.

As fibras foram depois utilizadas para estabilizar emulsões Pickering óleo-em-água. Os resultados mostraram que secagem, moagem e desintegração foi a melhor combinação de pré-tratamentos em termos da redução do diâmetro das fibras, permitindo obter CMF após a homogeneização. As polpas contendo CMF foram utilizadas para a produção de emulsões Pickering a diferentes razões O/W (20/80-70/30 wt.%) e teores sólidos de polpa na fase aquosa (PSC) (1,0-4,8 wt.%). O óleo foi disperso na fase aquosa com um homogeneizador rotor-estator para se obter uma fase de emulsão homogénea. Os melhores resultados de estabilidade obtiveram-se quando o alho francês pré-tratado foi homogeneizado a alta consistência com 6 passagens de HPH a 600 bar. Por outro lado, a alface pré-tratada foi apenas centrifugada.

Após 48 h, foi observada por inspeção visual pelo menos uma formulação para cada razão O/W com um índice de emulsão (EI) superior a 92 wt.%, demonstrando a viabilidade da utilização de resíduos de alho francês e alface para a produção de emulsões Pickering. Além disso, os resultados indicaram que o aumento do PSC resultou numa fase de emulsão mais elevada.

Neste trabalho, foram produzidas pela primeira vez emulsões Pickering estáveis contendo celulose existente em polpa de alho francês e alface. Estes resultados poderão contribuir para uma economia circular, pela utilização de produtos de origem biológica, e poderão abrir novos nichos de mercado e modelos de negócio.

Palavras-chave: emulsões Pickering; resíduos agrícolas; celulose; microfibras de celulose; aplicação alimentar

Declaration

I hereby declare, under word of honour, that this work is original and that all non-original contributions are indicated, and due reference is given to the author and source.

Porto, July 4, 2022

Mariana Marques Maio Pereira

Index

List of Figures

List of Tables

Notation and Glossary

G'	storage modulus	Pa
G''	loss modulus	Pa
a	polymer-solvent parameter	
AR	aspect ratio	
C	concentration	g m^{-3}
CD	cationic demand	meq g^{-1}
EI	emulsifying index	wt.%
GP	gel point	kg m^{-3}
H	height	m
k	empirical constant	
K	polymer-solvent parameter	mL g^{-1}
l	pathlength	m
m	weight	g
N	normality	eq m^{-3}
PD	polymerization degree	monomeric units
r	solid particle radius	m
t	time	s
T	temperature	°C
UV_{abs}	UV-visible absorbance	
V	volume	m^3

Greek Letters

θ	contact angle	°
$\dot{\gamma}$	shear rate	s^{-1}
$[\eta]$	limiting viscosity number	
Δ	variation	
γ	shear strain	%
ε	absorptivity of biomass at specific wavelength	L g^{-1} cm^{-1}
η	viscosity	Pa s
τ	shear stress	Pa
ω	angular frequency	rad s^{-1}

Indexes

*	maximum
0	initial
DS	dried sample
F	sediment
O	reference
RM	raw material
s	sample

List of Acronyms

BC	Bacterial Cellulose
C	Centrifugation
CED	Cupri-ethylenediamine
CLSM	Confocal Laser Scanning Microscopy
CMF	Cellulose Microfibres
CNC	Cellulose Nanocrystals
CNF	Cellulose Nanofibres
D	Disintegration

DS	Disintegration and drying
DSM	Disintegration, drying, and milling
FEUP	Faculty of Engineering University of Porto
HC	High-consistency
HPH	High-Pressure Homogenization
HPLC	High-Performance Liquid Chromatography
i3S	Instituto de Investigação e Inovação em Saúde
LC	Low-consistency
LSRE-LCM	Laboratory of Separation and Reaction Engineering - Laboratory of Catalysis and Materials
LVE	Linear Viscoelastic Region
M	Milling
NC	Nanocellulose
O/W	Oil/water
OM	Optical Microscopy
PSC	Pulp's solid content in the aqueous phase
S	Drying
SEM	Scanning Electron Microscopy
SFA	Saturated fatty acids
SM	Drying and milling;
SMD	Drying, milling, and disintegration
TFA	Trans fatty acids
UCM	Complutense University of Madrid
UFA	Unsaturated fatty acids

1 Introduction

1.1 Framing and presentation of the work

Agriculture, food industries, and grocery stores currently produce a large amount of waste, such as discarded fruits and vegetables, peels, and fruit trimming. These residues are mostly being burnt or tossed away as waste, which may cause several environmental problems. In areas where waste is accumulated without treatment, there is production of nitrous oxide, methane, sulphur dioxide, and smoke. If residues are burnt as an alternative, there is emission of carbon dioxide, contributing to atmospheric pollution (Jimenez-Lopez et al., 2020; Rao & Rathod, 2018).

Agricultural residues constitute a great source of lignocellulosic matter, which is composed of cellulose, hemicellulose, and lignin (Mateo et al., 2021). Cellulose is a renewable biopolymer, largely synthetized by plants, and can be used to produce cellulose nanofibres (CNF) and microfibres (CMF). CNF and CMF have unique properties that, along with their sustainable nature, grant them applications in broad areas such as paper and cardboard, water treatment, and food (Negro et al., 2020). Thus, the valorisation of food waste is of great interest to prevent environmental damage while promoting a circular economy through the production of high value-added products such as CNF and CMF.

On the other hand, in recent years, consumers have been looking for healthier food-products of natural origin as an alternative to synthetic additives (Costa et al., 2018). Due to CNF's amphiphilic properties, it can act as a stabilizer for Pickering emulsions. Pickering emulsions use solid particles to stabilize the oil/water (O/W) interface. By forming a physical barrier around the continuous phase droplets, they grant more stability against coalescence than traditional emulsions stabilized by surfactants.

The most common method used to produce emulsion-grade products with increased hardness and longer shelf life is the hydrogenation of vegetable oils, i.e., the hydrogenation of unsaturated fatty acids (UFA) into saturated fatty acids (SFA). This process involves the addition of hydrogen atoms to cis UFA by eliminating their double carbon bonds, and as a result, SFA are obtained. However, during this process, some of the cis bonds transform into trans bonds, creating trans-fatty acids (TFA) instead of SFA. The ingestion of TFA is harmful to health since it decreases high-density lipoprotein cholesterol ("good" cholesterol) and increases low density lipoprotein cholesterol ("bad" cholesterol) in the blood, increasing the risk of heart disease (Marchand, 2010). Pickering emulsions are a low-calorie substitute for SFA and UFA used in the food industry as they can increase product hardness while using low oil contents (Sanchez-Salvador et al., 2019).

The objectives of this Master dissertation are first, to obtain mechanical cellulose micro/nanofibres from leek and lettuce residues, and second, to apply them for the stabilization of Pickering emulsions formulations, with reduced fat, for future application in the food area.

1.2 Contribution of the author to the work

The work detailed in this dissertation was developed at Laboratory of Separation and Reaction Engineering – Laboratory of Catalysis and Materials (LSRE-LCM), from Faculty of Engineering University of Porto (FEUP), in collaboration with the Cellulose, Paper, and Advanced Water Treatments research group, from Complutense University of Madrid (UCM).

At UCM, cellulose micro/nanofibres were obtained, characterized, and tested as Pickering emulsions stabilizers to determine the optimal conditions for their obtention. The cellulose treatment was proposed by Professor Blanco. The fibres were obtained in collaboration with PhD student Jose Sanchez-Salvador from leek and lettuce residues by high-pressure homogenization (HPH), and raw materials were characterised by determining ash, extractives, insoluble and soluble lignin content. Additionally, PhD student Jose Sanchez-Salvador characterized lettuce pulps from the C-HPH-1-Lettuce homogenization sequence. Hemicellulose and cellulose content were determined by the FQPIMA research group. The pre-treatments, remaining characterization of the pulps, and Pickering emulsions production were performed by the author.

At FEUP, different formulations of Pickering emulsions were produced and characterized with the cellulose micro/nanofibres obtained at UCM. Confocal Laser Scanning Microscopy (CLSM) was performed by Instituto de Investigação e Inovação em Saúde (i3S). Scanning Electron Microscopy (SEM) analysis of the raw materials was done by Doctor Yaidelin Manrique. Contact angle determination of the pulps and rheological characterization of emulsions were conducted in collaboration with M.Eng. Ana Rita Fernandes and Doctor Margarida Brito, respectively. The author performed emulsification of all formulations along with the remaining characterization.

1.3 Organization of the dissertation

This dissertation is organized into six chapters.

Chapter 1 introduces the framing and presentation of the work (Section 1.1) developed as well as its main objectives. Additionally, the contributions of the author to the work (Section 1.2) are stated.

Chapter 2 explains all the theoretical concepts relevant for understanding this dissertation's later chapters. To that end, three main topics are addressed: cellulose and nanocellulose (Section 2.1), Pickering emulsions (Section 2.2), and applications of cellulose fibres in Pickering emulsions (Section 2.3).

Chapter 3 presents all the materials and methods used to obtain the results of this study, namely for production of cellulose fibres (Section 3.1), characterization of raw materials and cellulose fibres (Section 3.2), conditions of cellulose fibres production for Pickering emulsions application (Section 3.3), and Pickering emulsions (Section 3.4).

Chapter 4 focuses on the results obtained during the production of cellulose fibres (Section 4.1), characterization of raw materials and cellulose fibres (Section 4.2), determination of the conditions of

cellulose fibres production for Pickering emulsions application (Section 4.3), and final application to Pickering emulsions (Section 4.4). It also includes their interpretation and discussion.

Chapter 5 summarizes the main conclusions obtained throughout this study.

Finally, Chapter 6 describes the objectives achieved (Section 6.1), other work carried out (Section 6.2) during the course of the dissertation, and the current limitations and future work (Section 6.3) suggestions.

2 Context and State of the Art

2.1 Cellulose and nanocellulose

Nanocellulose (NC) has emerged over the last decade as a promising material. From 2006 to 2018, there was a consistent yearly increase in the number of scientific publications and patent documents on the subject. Using Web of Science, Current Contents Connect, BIOSIS Previews, and MELINE® databases, a 3163, 2277, 1286, and 995 document growth was registered, respectively (Negro et al., 2020). As the name indicates, it presents at least one dimension in the nanometre range (1–100 nm) (Blanco et al., 2018).

Because of its nano size, NC has unique properties such as high surface area and consequent high capacity for interaction with the surrounding medium (e.g., water, inorganic, organic, and polymeric compounds), amphiphilicity, lightweight, and high strength (Balea, 2017; Negro et al., 2020).

NC is obtained from cellulose fibres by reducing its diameter or both its diameter and length through appropriate mechanical, chemical, and/or enzymatic treatments (Sanchez-Salvador et al., 2021). Thus, in addition, NC presents inherent properties related to cellulose, such as biodegradability, biocompatibility, non-toxicity, and sustainability (Negro et al., 2020).

Cellulose is one of the most abundant and renewable natural biopolymers synthesized by plants, fungus, bacteria, and tunicates, which are small marine animals. It is essential as the primary structural component of plants, along with hemicellulose and lignin (Balea, 2017).

Cellulose consists of a linear chain of *n* glucose molecules linked through β-1,4-glycosidic bonds. It is represented by the chemical formula $(C_6H_{10}O_5)_n$ and the molecular structure of Figure 2.1 (Blanco et al., 2018). Due to β-1,4-glycosidic bonds, the glucose molecules turn into anhydroglucose units, commonly referred to as the monomer of the cellulose polymer (Nechyporchuk et al., 2016). Therefore, *n* corresponds to the number of anhydroglucose units in the polymer chain, i.e., the polymerization degree (PD) (Blanco et al., 2018).

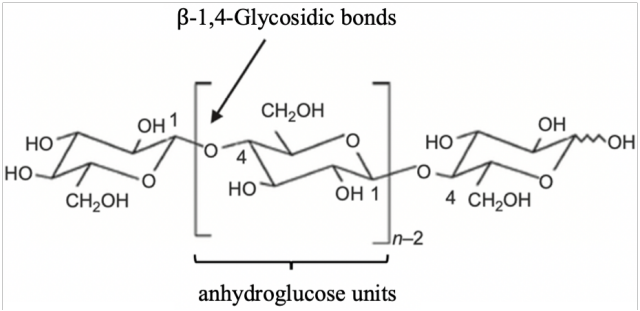

Figure 2.1. Molecular structure of cellulose. *Adapted from Blanco et al. (2018).*

Each monomer unit has three hydroxyl groups that form intra-chain hydrogen bonds and stabilize the resulting linear chain by forming elementary fibres (Rashid & Dutta, 2020). Each elementary fibre can be

composed of 30 to 100 cellulose chains, have a diameter of 2 to 20 nm, and a few micrometres in length. Also, it has regions where cellulose chains are arranged in an ordered manner (crystalline), conferring high strength, and others in a disordered manner (amorphous), granting elasticity. As Figure 2.2 represents, these elementary fibres form microfibres, which in turn form cellulose fibres (Rojas et al., 2015).

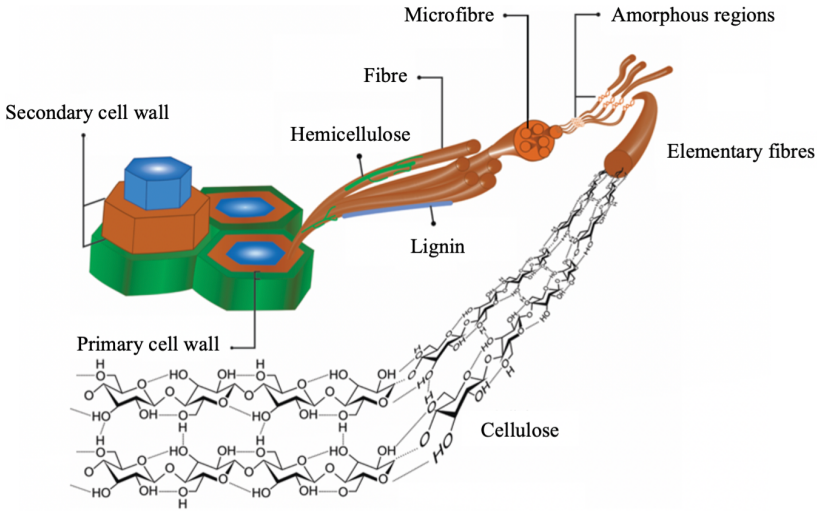

Figure 2.2. Hierarchical structure of cellulose extracted from plants. *Adapted from Rojas et al. (2015).*

2.1.1 Types of nanocellulose

According to the source and treatment performed on the cellulose fibres, the dimensions, functions, and properties of NC highly differ. Thus, three main types of NC can be distinguished, as established by the ISO/TS 20477:2017 standard: cellulose nanofibres (CNF), cellulose nanocrystals (CNC), and bacterial cellulose (BC).

CNF are obtained by mechanical fibrillation of the cellulose fibres. They are composed of elementary fibres or bundles of elementary fibres with amorphous and crystalline parts. CNF's diameters typically range from 3 to 100 nm with lengths up to 100 μm. Consequently, they have a large aspect ratio (AR > 200), defined as the length to diameter ratio (Blanco et al., 2018; ISO, 2017).

On the other hand, CNC are typically extracted by acid hydrolysis. This chemical treatment enables the cleavage of the amorphous regions of the elementary fibres, leaving only the crystalline part. Therefore, compared to CNF, CNC presents smaller diameters (3-50 nm) and 100 nm to several μm in length. This results in a lower aspect ratio (2 < AR < 100) (ISO, 2017; Rojas et al., 2015).

The last type of NC cannot be extracted from plants. BC is synthesized by aerobic bacteria and obtained through biotechnological processes. BC is obtained and interlinked, forming membranes or spheres depending if incubation is in static or agitated culture, respectively (Blanco et al., 2018).

2.1.2 Source of cellulose

NC can be isolated from almost all biomass that contains cellulosic fibres. Wood plants are the most studied group and a common CNF/CNC extraction source. Both types of NC can also be obtained from recycled

pulps and non-wood plants, such as seed fibres (e.g., cotton, coir), bast fibres (e.g., flax, hemp, jute, ramie), and grasses (e.g., bagasse, bamboo) (Nechyporchuk et al., 2016).

Moreover, the viability of extracting cellulose from agricultural waste is becoming a research focus. Large amounts of biomass are being burnt and tossed away as waste. Using them to produce high value-added products such as NC would traduce in environmental benefits such as reducing waste and promoting a circular economy (Jimenez-Lopez et al., 2020; Sanchez-Salvador et al., 2021).

Some of the published alternatives include residues from the banana rachis (Zuluaga et al., 2007) and peel (Tibolla et al., 2019), corn stalk (Balea et al., 2016), pineapple leaves (Araya-Chavarría et al., 2022), onion skin (Rhim et al., 2015), and apple pomace (Lu et al., 2020). Zhang et al. (2019) studied the extraction of cellulose from lettuce peel through a chemical process that consisted of NaOH alkali solution treatment, $NaClO_2$ bleaching, and then sulfuric acid hydrolysis to obtain CNC. To the best of the author's knowledge, NC extraction from leek leaves has not been reported to this date.

2.1.3 Production of CNF

The choice between the desired type of NC and what treatments to perform is essentially based on the intended application. For food products, where consumer safety is the main concern, it is essential to avoid chemical treatments since they typically use substances that might be toxic. Thus, mechanical treatments to obtain CNF are preferred (Lu et al., 2020).

One of the most used processes to produce CNF is high-pressure homogenization (HPH) (Balea et al., 2016; Zuluaga et al., 2007). However, there are others, including microfluidization (Araya-Chavarría et al., 2022), grinding (Lu et al., 2020), and ultrasonication (Rhim et al., 2015). HPH is performed using a homogenizer that produces a homogeneous size distribution of diluted CNF. As Figure 2.3 schematically represents, diluted cellulose fibres are pumped at high pressure and low velocity while the homogenization valve opens and closes in a cyclic motion. When the suspension passes through the small gap between the valve and the seat, there is a rapid increase in velocity and pressure drop to atmospheric conditions. Consequently, the high shear and impact forces generated ensure the decrease of cellulose's size and PD reduction (Blanco et al., 2018; Rojas et al., 2015).

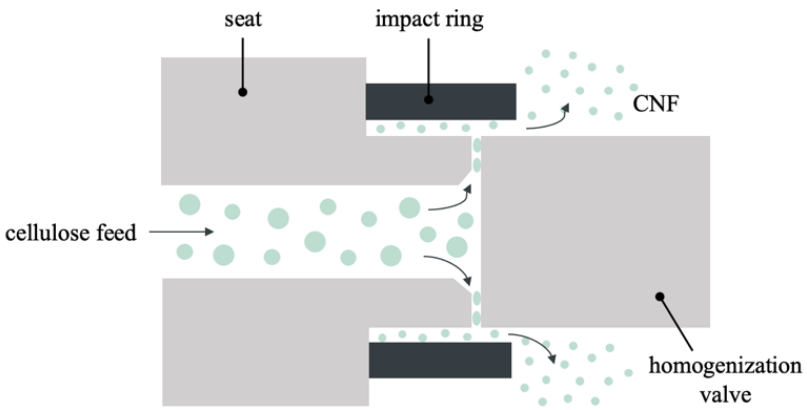

Figure 2.3. Representation of the production of CNF by HPH.

Although this is an efficient technique to produce CNF at laboratory scale, there are associated problems, such as high energy demand to achieve higher fibrillation, and equipment clogging if the feed's cellulose fibres are too large or not properly diluted (Rojas et al., 2015). Thus, chemical, mechanical, biological, or combined pre-treatments are typically carried out to make the subsequent fibrillation easier and less expensive.

To obtain chemically unmodified CNF, mechanical pre-treatments should be applied. However, while facilitating fibre separation, some mechanical techniques have been reported to produce a highly heterogeneous product (Sanchez-Salvador et al., 2021).

2.1.4 Applications of CNF

The desirable properties of NC and its sustainable nature have attracted the researcher's attention in vast areas of applications. To name a few: (i) the paper and cardboard industry, where NC acts as a strengthening agent for recycled products; (ii) water treatment, by retaining certain pollutants on its surface; (iii) the construction industry, in which NC improves the mechanical properties of cement composites and makes them more resistant (Negro et al. 2020).

The food industry is another area of application of cellulose nanofibres. NC can be used as a functional food additive, to prepare reduced-fat formulations of high-density foods (e.g., cheese and hamburgers), and in food packaging, either to produce biodegradable coatings and films or as an active material with antimicrobial and antioxidant properties. Moreover, NC can act as a green stabilizer and emulsifier for salad dressings, whipped toppings, sauces, foams, soups, among others (Blanco et al. 2018; Negro et al. 2020).

2.2 Pickering emulsions

Emulsions are systems of two immiscible liquids where one liquid is dispersed in the other as droplets. They are usually prepared under an external energy source, producing small droplets with a large total interfacial area. However, since the liquids are immiscible, they tend to separate at thermodynamic equilibrium. Once external shearing stops, the droplets tend to coalesce to lower the total interfacial area, reverting to the original state of phase separation (Sun et al., 2022).

Low-molecular-weight surfactants or surface-active polymers are traditionally used to ensure the long-term stability of emulsion-based products. Their amphiphilic properties enable them to adsorb at the oil/water (O/W) interface, reduce the interfacial tension, and prevent the coalescence of droplets (Gonzalez Ortiz et al., 2020).

Pickering emulsions were introduced at the beginning of the 20th century by Ramsden and Pickering as a pioneering concept. Instead of the traditional emulsifiers, they use solid particles that form a thick barrier at the O/W interface. Thus, by acting as an obstacle, they grant higher stability against the coalescence of droplets than traditional surfactants (Pickering, 1907).

2.2.1 Emulsification process

Pickering emulsions production relies essentially on batch processes, namely rotor-stator homogenization. Rotor-stator homogenizers consist of a rotating shaft (the rotor) inside a stationary hollow casing (the stator). The rotor's rotation creates a pressure differential, drawing the fluid in and out the small space between the rotor and the stator. Due to the extreme change in velocity that happens in the gap, the fluid is subjected to high shear forces that promote the reduction of emulsions' droplet size (*Rotor-Stator Homogenization*).

The advantages of rotor stator homogenization include low operating cost, easy set-up, rapidity of emulsification, and the production of small volumes. However, it has some drawbacks such as possible lack of emulsion phase uniformity, temperature increase, limit energy input, production of large-size heterogeneous droplets, and difficult scale-up (Albert et al., 2019).

2.2.2 Types of Pickering emulsions

The solid particles used to stabilize Pickering emulsions also have amphiphilic properties, i.e., the ability to be partially wetted by both liquids. This dual wettability is an important characteristic of emulsion stabilizers; if the particles were fully wetted by one of the phases, they would remain dispersed in that phase, not stabilizing the emulsion (Gonzalez Ortiz et al., 2020).

Two types of Pickering emulsions can be distinguished: oil-in-water and water-in-oil emulsions. The oil-in-water emulsions are characterized by the formation of oil droplets in a continuous phase, the aqueous phase. The opposite behaviour occurs for water-in-oil emulsions. The type of emulsion formed depends mainly on the wettability of the particles, which can be characterized by the three-phase contact angle measured through the water phase (θ). As Figure 2.4 illustrates, predominantly hydrophilic particles, with $\theta < 90°$, usually stabilize oil-in-water emulsions, while hydrophobic particles, with $\theta > 90°$, lead to water-in-oil emulsions (Binks & Lumsdon, 2000).

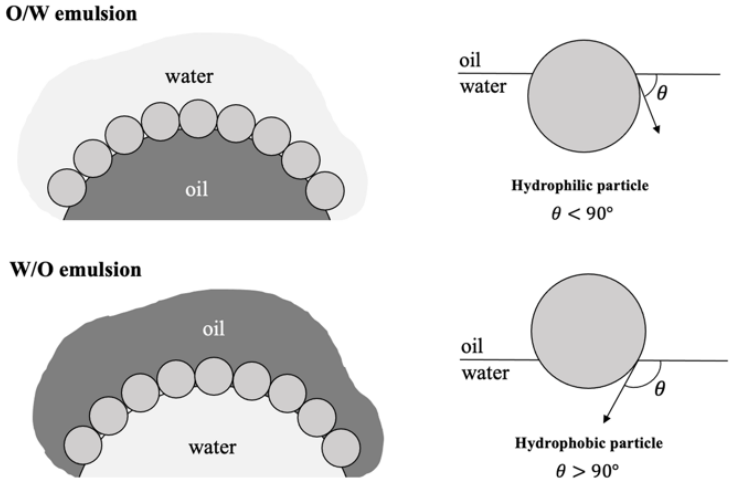

Figure 2.4. Schematic representation of the types of Pickering emulsions and respective three-phase contact angle (θ).

2.2.3 Emulsion stability

Since the fundamental difference between traditional and Pickering emulsions is that the latter uses solid particles as the emulsifier instead of surfactants, the stability of the Pickering emulsions depends highly on the properties of the solid particles. Thus, in addition to wettability, stability is influenced by factors such as particle concentration, size, and shape (Albert et al., 2019; Gonzalez Ortiz et al., 2020).

(i) *Particle concentration*: when the stabilizer is at low concentrations, instability is often observed from the lack of particles to encapsulate all droplets. The increase in the concentration of the solid particles leads to more particles being available to adsorb at the O/W interface, and the emulsion stability tends to be proportionally higher. Simultaneously, the average droplet size decreases since more particles are available to cover a larger surface area (Gonzalez Ortiz et al., 2020; Ribeiro et al., 2022).

(ii) *Particle size:* to stabilize a Pickering emulsion, particles should be, ideally, one order of magnitude smaller in diameter than the desired emulsion droplet size (Albert et al., 2019; Sun et al., 2022).

(iii) *Particle shape*: Pickering emulsions can be stabilized with spherical and non-spherical particles (e.g., rods, fibres, cubes). According to the geometry of the particles, the stabilization mechanism may differ (Albert et al., 2019).

2.2.4 Applications of Pickering emulsions

Pickering emulsions can be used as an alternative to traditional emulsions in most applications. Besides showing long-term stability, Pickering emulsions avoid some of the adverse effects caused by the use of surfactants, such as skin irritation, environmental pollution, and metabolic syndrome (Lu et al., 2018). Thus, their “surfactant-free” character makes them advantageous, especially in pharmaceutics (e.g., better encapsulation for drug delivery), cosmetics (e.g., less greasy sunscreen), and food (e.g., low-calorie alternative to trans and saturated fats) (Ribeiro et al., 2021; Sanchez-Salvador et al., 2019; Sun et al., 2022).

2.3 Application of cellulose fibres in Pickering Emulsions

Silica (Duan et al., 2009), clay particles (Guillot et al., 2009), and titanium oxides (Chen et al., 2007) are solid particles used as stabilizers for Pickering emulsions. However, their application in food-grade products is limited because these emulsifiers are not biocompatible or biodegradable.

CNF are promising natural and sustainable nanoparticles that some authors have studied in recent years. Costa et al. (2018) stabilized Pickering emulsions with CNF from banana peels, produced by HPH and ultrasonication, and pre-treated with alkaline treatment and enzymatic hydrolysis. Li et al. (2019) used CNF from oil palm empty fruit bunch, produced by HPH, and pre-treated with soda pulping, bleaching, and TEMPO oxidation. Also, He et al. (2020) used CNF as a Pickering stabilizer obtained from bamboo shoot by HPH with a pre-alkaline treatment.

The success of CNF as a stabilizer for Pickering emulsions is essentially due to its amphiphilic nature. As Figure 2.5 shows, CNF has a hydrophobic face and a hydrophilic edge, enabling the nanofibres to have an efficient role at the O/W interface and stabilize the emulsion (Sanchez-Salvador et al., 2019). Since CNF has longer length than the droplets' diameter, the particles promote the formation of a network instead of individual droplets, which can result in higher stability (Lu et al., 2018).

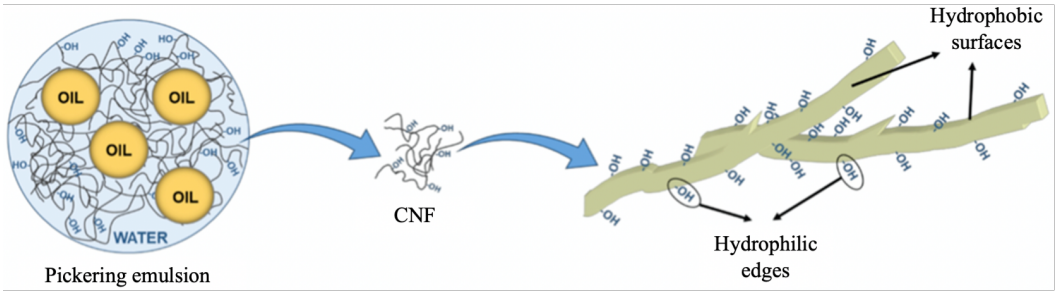

Figure 2.5. CNF as a stabilizer for Pickering emulsions. *Adapted from Sanchez-Salvador et al. (2019).*

However, none of the mentioned studies produced Pickering emulsions using chemically unmodified CNF, as required by food applications. Another derivative of cellulose fibres are cellulose microfibres (CMF), composed of several elementary fibres (Figure 2.2) and with diameters within the micro range. CMF have also shown potential as a chemical unmodified Pickering stabilizer.

Sanchez-Salvador et al. (2019) studied the stability of emulsions at different O/W ratios and CMF concentrations, using CMF extracted from cotton without chemical treatments. Lu et al. (2020) used CMF present in apple pomace, obtained by wet-milling mechanical treatment, to prepare emulsions at a constant O/W ratio (50/50 wt.%) and studied the influence of particle size and CMF concentration. Both studies of Sanchez-Salvador et al. (2019) and Lu et al. (2020) indicated that higher concentrations of CMF resulted in a more entangled network that increased the emulsion stability. Furthermore, Lu et al. (2020) also observed that particle size reduction resulted in emulsion droplets with smaller dimensions and more stability at the same CMF concentration.

3 Materials and Methods

3.1 Production of cellulose fibres

In this Master dissertation, leek and lettuce, which are the source of cellulose fibres, were kindly provided by a local greengrocer's shop from Madrid, Spain. The raw materials were initially mechanically pre-treated and then further fibrillated by high-pressure homogenization (HPH).

3.1.1 Pre-treatment selection

Before HPH, leek and lettuce residues were submitted to pre-treatments to obtain chemically unmodified cellulose fibres. Two types of mechanical techniques were tested: disintegration (D) and milling (M). Drying (S) of the samples in an oven was also considered.

The disintegration of the raw materials with distilled water was done in a 212023 Princess Power Blender (Princess, Breda, The Netherlands) at 14 000 rpm for 1 min and 18 000 rpm for 2 min. The residues were milled in a CT 293 Cyclotec Mill (Foss, Hilleroed, Denmark) after being oven-dried at ~100 °C for 24 h.

Different pre-treatment combinations were considered and named according to the order of each process. Each process was named according to:

- **(D)** disintegration;
- **(DS)** disintegration and drying;
- **(DSM)** disintegration, drying, and milling;
- **(SM)** drying and milling;
- **(SMD)** drying, milling, and disintegration.

To prevent fermentation, 6 to 8 droplets of biocide (glutaraldehyde 2 wt.%) were added to the pulps. All combinations were tested for leek and lettuce. HPH of samples after the corresponding combination of pre-treatments was performed at 600 bar and 1 pass in a laboratory homogenizer NS1001L PANDA 2K-GEA (GEA Niro Soavy, Parma, Italy). The selection of the optimal combination was made according to optical microscopy (OM) analysis, maximum consistency attainable after 1 pass, and overall characteristics of the HPH procedure.

Each sample is identified in this work with "pre-treatment-HPH-number of HPH passes-raw material" [e.g., D-HPH-1-Lettuce corresponds to disintegrated (**D**-HPH-1-Lettuce) lettuce (D-HPH-1-**Lettuce**) with 1 pass of HPH (D-**HPH-1**-Lettuce)].

3.1.2 High-Pressure Homogenization

Mechanical fibrillation of the raw materials pre-treated according to the chosen optimal combination was carried out at 600 bar and until 9 passes in the laboratory homogenizer. The different homogenization sequences performed are presented below. For lettuce, an additional pre-treatment of centrifugation I in a SIGMA 3-16P centrifuge (SIGMA Laborzentrifugen, Osterode am Harz, Germany) at 4 500 rpm for 20 min was tested before HPH in one of homogenization sequences:

- HPH-9-LC-Leek: 9 passes of low consistency SMD leek at 600 bar;
- HPH-9-HC-Leek: 9 passes of high consistency SMD leek at 600 bar;
- HPH-9-LC-Lettuce: 9 passes of low consistency SMD lettuce at 600 bar;
- C-HPH-1-Lettuce: centrifugation (C) of SMD lettuce and then 1 pass at 600 bar.

3.2 Characterization of the raw materials and cellulose fibres

Characterization of the raw materials and cellulose fibres was done considering three main aspects: (i) compositional characterization, with the determination of the raw materials solids content (consistency), the chemical composition of the raw materials and centrifugated lettuce (ash, extractives, insoluble and soluble lignin, cellulose, and hemicellulose content), and the content of carboxylic groups; (ii) consistency throughout HPH; (iii) morphologic characterization, with OM analysis and determination of aspect ratio (AR), polymerization degree (PD), transmittance, and cationic demand (CD) throughout HPH.

3.2.1 Chemical compositional characterization

3.2.1.1 Ash content

The ash content, i.e., the inorganic composition of the raw materials, was determined by calcination at 525 °C in a muffle furnace, according to TAPPI T211. The analysis was performed on D-HPH-0-Leek and -Lettuce. Before calcination, the suspensions were oven-dried at ~70 °C for 12 h and their mass was registered (m_{dry}). The mass of ashes was also registered (m_{ash}). The ash content was estimated by

$$\text{ash content (wt.\%)} = \frac{m_{\mathrm{ash}}}{m_{\mathrm{dry}}} \times 100 \quad \textbf{(3.1)}$$

3.2.1.2 Extractives content

The extractives content was determined by Soxhlet extraction according to TAPPI T204. The raw materials and centrifugated SMD-HPH-0-Lettuce were oven-dried at ~70 °C for 12 h, milled, and then the mass was registered (m_{RM}). The mass of the extraction flasks was also measured (m_{flask}) and then they were filled with 150 mL of the solvent, acetone. The Soxhlet extraction was performed for 3 h. The flasks with the extractives were oven-dried at ~65 °C for 12 h, and the respective mass was registered (m_{extract}). The extractives content was determined by

$$\text{extractives content (wt.\%)} = \frac{m_{\mathrm{extract}} - m_{\mathrm{flask}}}{m_{\mathrm{RM}}} \times 100 \quad \textbf{(3.2)}$$

3.2.1.3 Insoluble and soluble lignin, cellulose, and hemicellulose content

The extractives free samples, collected after Soxhlet extraction, were dried at ~65 °C for 12 h. Insoluble and soluble lignin, cellulose, and hemicellulose content were measured according to NREL/TP-510-42618 standard. 300 mg of the dried samples (m_{DS}) were hydrolysed with 4.90 g of 72 wt.% H_2SO_4 for 1 h in a water bath at 30 °C. The samples were then diluted to a 4 wt.% consistency by adding 84 g of deionized

water and placed in an autoclave for 1 h at 121 °C. Then, they were vacuum filtered. Deionized water was added to ensure that all the remaining solids of the samples were transferred to the filters.

Insoluble lignin content was obtained from

$$\text{insoluble lignin content (wt.\%)} = \frac{m_{\text{dry}} - m_{\text{ash}}}{m_{\text{DS}}} \times 100 \quad \textbf{(3.3)}$$

according to TAPPI T211. To determine the respective m_{dry} and m_{ash}, sediments were oven-dried at ~70 °C for 12 h and calcinated at 525 °C in a muffle furnace.

The filtrate was diluted with ionized water. The dilution is determined from

$$\text{dilution} = \frac{V_{\text{sample}} + V_{\text{solvent}}}{V_{\text{sample}}} \quad \textbf{(3.4)}$$

Its UV-visible absorbance (UV_{abs}) was measured using a spectrophotometer uniSPEC 4 UV-Visible (LLG, Meckenheim, Germany) at a wavelength of 240 nm.

Soluble lignin content was obtained from

$$\text{soluble lignin content (wt.\%)} = \frac{\text{UV}_{\text{abs}}\, V_{\text{filtrate}}\, \text{dilution}}{\varepsilon\, m_{\text{DS}}\, l} \times 100 \quad \textbf{(3.5)}$$

where V_{filtrate} is the volume of filtrate (86.73 mL), ε is the absorptivity of biomass at specific wavelength (12 L g^{-1} cm^{-1}), and l is the pathlength of the UV-visible cell (1 cm).

Finally, the filtrate was neutralized with $CaCO_3$ and filtered through 0.2 µm filters. Its analysis by High-Performance Liquid Chromatography (HPLC) enabled obtaining the cellulose and hemicellulose content.

3.2.1.4 Carboxylic groups

The content of carboxylic groups in the raw materials was determined by conductometric titration. Samples of D-HPH-0-Leek and -Lettuce were used for this analysis.

5 mL of NaCl (0.01 M) were added to 0.2 g, in dry weight (m_{dry}), of each cellulose suspension. Deionized water was then added up to a total volume of 60 mL. The pH of this dilution was adjusted to ~2.8 using HCl. Titration in continuous agitation was performed with NaOH 0.05 N (N_{NaOH}) after placing a conductivity probe in the sample. For each 0.2 mL (leek) or 0.5 mL (lettuce) of NaOH added, the conductivity of the dilution was registered. A curve of conductivity (µS cm^{-1}) vs. NaOH volume (mL) was represented. Figure 3.1 shows the typical curve that is obtained.

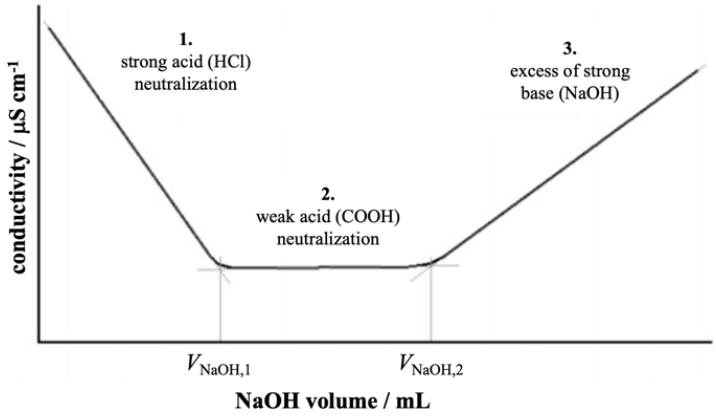

Figure 3.1. Typical conductivity versus NaOH volume curve obtained from titration of a strong base (NaOH) to a mixture of a strong acid (HCl) and a weak acid (carboxylic groups). *Adapted from Balea (2017).*

The ascending and descending branches of the curve were linearly adjusted and the constant conductivity value from the weak acid neutralization was registered. $V_{\mathrm{NaOH},1}$ and $V_{\mathrm{NaOH},2}$ were determined from the intersection of the three curves, as shown in Figure 3.1

Therefore, the content of carboxylic groups per gram of dried raw material was determined from

$$\frac{\mathrm{COOH\ (mmol)}}{\mathrm{dried\ sample\ (g)}} = \frac{\left(V_{\mathrm{NaOH},1} - V_{\mathrm{NaOH},2}\right) N_{\mathrm{NaOH}}}{m_{\mathrm{dry}}} \quad \textbf{(3.6)}$$

3.2.2 Consistency throughout HPH

The consistency, i.e., the solid content of each pulp, was obtained from

$$\mathrm{consistency\ (wt.\,\%)} = \frac{m_{\mathrm{dry}}}{m_{\mathrm{humid}}} \times 100 \quad \textbf{(3.7)}$$

where m_{dry} is the mass of oven-dried pulps at ~70 °C for 12 h and m_{humid} is the mass of humid pulps.

3.2.3 Morphological characterization

3.2.3.1 Optical Microscopy analysis

A droplet of each pulp was diluted, put on a glass microscope slide, covered with a coverslip, and the cellulose micro/nanofibres were viewed under 5× magnification. An Axio Lab.A1 optical microscope and a colour microscope camera AxioCam ERc 5s (Zeiss Microscopy, Jena, Germany) were used, and image processing was performed with ImageJ software.

3.2.3.2 Aspect ratio

AR was determined from a simplified gel point (GP) methodology described by Sanchez-Salvador et al. (2021). GP is usually obtained from the derivative at the origin of an experimental curve of cellulose fibres' concentration (C_{AR}) versus ratio of sediment height (H_{f}) to initial suspension height (H_0). H_{f} and H_0 are measured as Figure 3.2 indicates. The following simplification is used to calculate GP

$$\mathrm{GP\ (kg\ m^{-3})} = \lim_{\frac{H_f}{H_0}\to 0}\left(\frac{dC_{AR}}{d\left(\frac{H_f}{H_0}\right)}\right) \approx \frac{C_{AR}(i) - C_{AR}(0)}{\left(\frac{H_f}{H_0}(i)\right) - \left(\frac{H_f}{H_0}(0)\right)} = \frac{C_{AR}(i)}{\left(\frac{H_f}{H_0}(i)\right)} \quad \textbf{(3.8)}$$

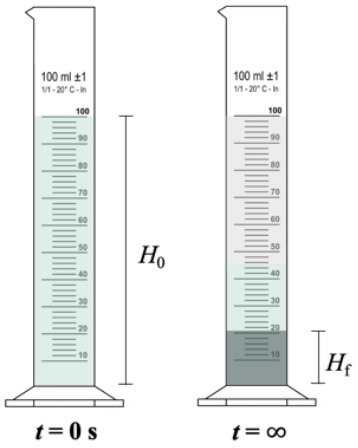

Figure 3.2. Representation of gel point sediment height (H_0) and initial suspension height (H_f) readings.

250 mL of diluted pulps at 0.1 wt.% were prepared with distilled water to determine GP. 200 µm of crystal violet 0.1 wt.% were added to visualize the sedimentation and the suspension was stirred for 5 min. The suspension was then left to settle in a graduated cylinder until complete sedimentation of the fibres.

After calculating GP, AR was determined according to

$$\mathrm{AR} = 6.0 \times \left(\frac{\mathrm{GP}}{1000}\right)^{-0.5} \quad \textbf{(3.9)}$$

assuming a 1500 kg m^{-3} density of cellulose fibres and the crowding number theory (Varanasi et al., 2013).

3.2.3.3 Polymerization Degree

PD was determined from the limiting viscosity number (intrinsic viscosity), according to the ISO 5351 standard (2010).

25 g of pulps at 1 wt.% were diluted in 25 g of cupri-ethylenediamine (CED) solution, and the elution time of the 0.5 wt.% sample was measured with a capillary viscometer. The elution time of a reference sample prepared with 25 g of distilled water and 25 g of CED was also determined.

The ratio of the elution time of cellulose fibres (t) and the reference (t_o) samples relates to the ratio of their viscosity (η and η_o, respectively) according to

$$\frac{\eta}{\eta_o} = \frac{t}{t_o} \quad \textbf{(3.10)}$$

For a certain ratio between η and η_o, the limiting viscosity number $[\eta]$ of the diluted sample was determined according to Martin's equation,

$$\log [\eta] = \log \frac{\eta - \eta_o}{\eta_o \, C_{PD}} - k \, [\eta] \, C_{PD} \quad \textbf{(3.11)}$$

where k is an empirical constant, which is 0.13 for the cellulose-CED system, and C_{PD} is the exact concentration of pulp-CED sample.

PD was then calculated using the Staudinger-Mark-Houwink equation,

$$[\eta] = K_{PD} \, PD^{a} \quad \textbf{(3.12)}$$

where K_{PD} and a are parameters specific to the polymer-solvent system. For the cellulose-CED system, K_{PD} and a vary according to

- if $PD < 950$, $K_{PD} = 0.42$ mL g^{-1} and $a = 1$;
- if $PD > 950$, $K_{PD} = 2.28$ mL g^{-1} and $a = 0.76$.

3.2.3.4 Transmittance

Each pulp was firstly diluted at 0.1 wt.% to determine the transmittance. The measurements were performed at a wavelength of 600 nm on a uniSPEC 4 UV-Visible spectrophotometer (LLG, Meckenheim, Germany). Distilled water was used as reference fluid.

3.2.3.5 Cationic demand

CD corresponds to the amount of cationic polymer needed by the pulps to reach the isoelectric point (zero potential) (Balea, 2017).

The measurements were performed by titration of 10 mL of the pulps at 0.1 wt.% with polyDADMAC 0.001 N cationic polymeric, using a Mütek PCD04 particle charge detector (BTG Instruments GmbH, Herrsching, Germany). The piston of this equipment moves vertically as the polymer is added, producing an electrical current that is measured by two electrodes (Cadena et al., 2009).

CD is given by

$$\text{CD (meq g}^{-1}) = \frac{V_{\text{polyDADMAC}} \, N_{\text{polyDADMAC}}}{V_{CD} \, C_{CD}} \quad \textbf{(3.13)}$$

where $V_{\text{polyDADMAC}}$ (mL) is the volume of polyDADMAC added during the titration, $N_{\text{polyDADMAC}}$ is the normality of the polymer (0.001 N), V_{CD} is the volume of the 0.1 wt.% pulp (10 mL), and C_{CD} (g mL^{-1}) is its concentration.

3.3 Conditions of cellulose fibres production for Pickering emulsions application

The raw materials used for emulsion preparation were sunflower oil, purchased from a local supermarket, chemically unmodified cellulose fibres, produced from residues of leek or lettuce, and distilled water. Emulsions were prepared as proof of concept of using pulps of leek and lettuce containing cellulose fibres as Pickering emulsion stabilizers. According to the results, conditions for fibre production were selected and the corresponding pulps were characterized by scanning electron microscopy (SEM) analysis and laser diffraction size distribution.

3.3.1 Leek and lettuce Pickering emulsions

Emulsions were prepared using pulps containing CMF/CNF collected after different numbers of passes of HPH for each homogenization sequence. The O/W ratio and the pulp's solid content in the aqueous phase (PSC) were fixed during these experiments. Table 3.1 summarizes the conditions considered.

Table 3.1. O/W ratio, PSC, and number of HPH passes considered for preparing Pickering emulsions for each homogenization sequence.

Homogenization sequence	O/W ratio / wt.%	PSC / wt.%	Number of HPH passes
HPH-9-LC-Leek	60/40	2.25	0 / 6 / 9
HPH-9-HC-Leek			0 / 3 / 6 / 9
HPH-9-LC-Lettuce	60/40	1.00	0 / 1 / 3 / 9
C-HPH-1-Lettuce			0 / 1

Emulsification was carried out in a rotor-stator homogenizer T 25 digital ULTRA-TURRAX (IKA, Staufen, Germany) at 16 000 rpm for 3 min. They were then stored in a graduated cylinder at room temperature.

For each raw material, the best homogenization sequence and the respective optimal number of HPH passes were chosen according to emulsion stability after 48 h. The volume of the water (V_{water}), oil (V_{oil}), and emulsion (V_{emulsion}) phases were measured and emulsion stability was expressed by the emulsifying index (EI), given by

$$\mathrm{EI}\ (\%) = \frac{V_{\mathrm{emulsion}}}{V_{\mathrm{total}}} \qquad \textbf{(3.14)}$$

where V_{total} is the total volume of the sample.

3.3.2 Scanning Electron Microscopy analysis

The chosen pulps for each raw material were analysed by SEM. They were oven-dried at ~100 °C for 3 h before the analysis. The dried samples were placed on pins with carbon tapes and observed on a desktop Phenom ProX Desktop SEM (Thermo Fisher Scientific, Massachusetts, EUA).

3.3.3 Laser Diffraction Size Distribution

Volume and number size distribution of the chosen pulps' cellulose fibres were obtained using a laser diffraction particle size analyser LS 230 (Beckman Coulter, California, EUA) by dispersing the samples in distilled water at room temperature. For each sample, three measurements were performed. The average diameters were determined for each distribution.

3.4 Pickering emulsions

The leek and lettuce pulps were used to produce Pickering emulsions. Firstly, a study on the optimal rotor-stator homogenizer conditions was performed. Then, emulsions were produced at different O/W ratios and PSC at fixed production conditions. Their stability was evaluated by visual inspection. An additional characterization was performed in terms of emulsion type (contact angle determination and drop test), stabilization mechanism [OM and Confocal Laser Scanning Microscopy (CLSM) images], and rheological properties.

3.4.1 Rotor-stator homogenizer conditions

The aqueous phase was initially dispersed for 1 min using a rotor-stator homogenizer Miccra D-9 (Miccra GmbH, Heitersheim, Germany) to ensure fibre dispersion. The oil was then injected through a feeding channel using a peristaltic pump at 240 rpm (~30.9 mL min^{-1}) and the injection time ($t_{\mathrm{injection}}$) was measured. The system was kept under stirring for an additional period (t_{stirring}) to ensure homogenization. The temperature was registered after dispersion and stirring ($T_{\mathrm{dispersion}}$ and T_{stirring}, respectively).

The adequate speed of the rotor-stator homogenizer and t_{stirring} conditions were initially determined by fixing the O/W ratio (40/60 wt.%) and PSC (3.0 wt.%) and varying the parameters in analysis. Leek pulp was used for this study. Table 3.2 indicates the analyses performed.

Table 3.2. Rotor-stator homogenizer conditions study: speed and time of stirring for a fixed O/W ratio and PSC.

O/W ratio / wt.%	PSC / wt.%	Speed / rpm	t_{stirring} / min
40/60	3.0	16 000	3
		16 000	$t_{\mathrm{injection}}$
		11 000	3
		11 000	$t_{\mathrm{injection}}$

According to emulsion stability after 48 h, expressed by the EI (Eq. 3.14), and variation of temperature ($\Delta T = T_{\mathrm{dispersion}} - T_{\mathrm{stirring}}$), the set of parameters was chosen. These conditions were considered for further stability study for both raw materials.

Pickering emulsions of leek at maximum PSC for O/W ratios from 70/30 to 20/80 wt.% were firstly analysed. Then, another set of emulsions was prepared at 40/60, 30/70, and 20/80 wt.% O/W ratios, with PSC ranging from 1.0 wt.% to maximum PSC. For lettuce, stability analyses were performed for O/W ratios

from 40/60 to 20/80 wt.% at PSC, ranging from 2.0 wt.% to maximum PSC. Table 3.3 summarizes the formulations tested for both leek and lettuce.

Table 3.3. Pickering emulsions stability study: O/W ratio and PSC for each raw material.

Raw material	O/W ratio / wt.%	PSC / wt.%
Leek	20/80	2.0 | 3.0 | 4.0 | 4.8*
	30/70	1.0 | 1.5 | 2.0 | 2.5 | 3.0 | 3.5 | 4.2*
	40/60	1.0 | 1.5 | 2.0 | 2.5 | 3.0 | 3.6*
	50/50	3.0*
	60/40	2.4*
	70/30	1.8*
Lettuce	20/80	2.0 | 3.0 | 4.0
	30/70	2.0 | 3.0 | 4.0
	40/60	2.0 | 3.0 | 3.8*

***Maximum PSC**

3.4.2 Pickering emulsion type

Pickering emulsion type was initially predicted by contact angle (θ) measurements on the raw materials pulps and then confirmed from drop test for all Pickering emulsions described in Table 3.3.

3.4.2.1 Contact angle

A sample of leek and lettuce pulps was dried in an oven at 100 °C for 3 h. The resulting powders were pressed into pellets with a diameter of 13 mm and a thickness of ~1 mm using a hydraulic press (PerkinElmer) at 10 tonnes. Measurements of the contact angle (θ) were performed through a sensible-drop method on an optical tensiometer Theta (Biolin Scientific). A droplet of distilled water (5 μL) was released on pellets surfaced using a high-precision injector and recorded with the high-speed video camara of the equipment. The contact angles for the left- and right-hand sides of the droplet were determined by the software One Attension using the Laplace-Young equation. Results are expressed as the average measurements for different repetitions of both θ.

3.4.2.2 Drop test

Emulsion type was reported by drop test. Two drops of each Pickering emulsion were added to the water and oil phases, respectively. According to their behaviour, emulsions were classified as oil-in-water or water-in-oil.

3.4.3 Visual inspection

Pickering emulsions of Table 3.3 were analysed visually to determine their stability. Images were captured after 1 h and 48 h of production. Stability was expressed by the EI, given by Eq. 3.14.

3.4.4 Stabilization mechanism

The stabilization mechanism used by cellulose fibres at the O/W interface was observed by OM and CLSM images.

3.4.4.1 Optical Microscopy analysis

The morphology of emulsions was observed by OM after production (day 0). A drop of emulsion was placed in a microscope slide, covered with a coverslip, and viewed under 10× magnification.

An Axiotech 100 HD optical microscope and a microscope camera AxioCam 105 colour (Zeiss Microscopy, Jena, Germany) were used. Image processing was performed with Zen (2.3 blue edition) software.

3.4.4.2 Confocal Laser Scanning Microscopy analysis

Emulsions were analysed by CLSC using a LEICA TCS-SP5 AOBS (Leica Microsystems, Germany) to visualize the cellulose fibres placement at the O/W interface. Each sample (3 mL) was stained with a mixture of fluorescent dyes dissolved in isopropyl alcohol (0.3 mL): Nile red at 0.1 w/v%, to dye the fibres, and Nile blue at 0.1 w/v%, to dye the oil droplets. The dyed emulsions were placed on a slide (40 μL) and excited at 488 nm (Nile red) and 633 nm (Nile blue). Image processing was performed using a LASX software and ImageJ.

3.4.5 Rheological Characterization

Rheological studies on viscous and viscoelastic behavior of Pickering emulsions were performed using a rheometer MCR 92 (Anton Paar, Graz, Austria) with a parallel plate. The zero gap was defined at 0.5 mm and the temperature at 20 °C for all measurements.

The viscosity curve, i.e., the viscosity of emulsions (η) in function of the shear rate ($\dot{\gamma}$), was measured for a shear rate range from 10 to 300 s^{-1}. The yield stress of emulsions was measured from the flow curve, i.e., the shear stress (τ) in function of $\dot{\gamma}$. The studied range of τ was from 1 to 50 Pa.

The linear viscoelastic region (LVR) was also determined by amplitude sweep, considering a shear strain (γ) in the range of 0.01 to 100 % and a fixed angular frequency (ω) of 10 rad s^{-1}. LVR region indicates the shear strain where the test can be performed without destroying the structure. The amplitude sweep tests are presented as a plot of storage modulus (G') and loss modulus (G'') in function of γ.

After the identification of LVR, a frequency sweep test was performed for ω in the range of 10 to 100 rad s^{1} and a fixed shear strain within the LVR. The frequency tests are presented as a plot of G' and G'' in function of ω.

4 Results and Discussion

4.1 Production of cellulose fibres

The first step of this work was to produce cellulose fibres, of micro or nano dimensions, from leek and lettuce residues. A novelty approach was the use of the full waste pulp without the previous extraction of the cellulose fraction. A combination of pre-treatments was initially selected and then each pre-treated pulp was fibrillated by high-pressure homogenization (HPH). Two homogenization sequences were performed for each raw material, considering different pulp conditions.

4.1.1 Pre-treatment selection

Leek and lettuce were submitted to different mechanical pre-treatments and combinations of pre-treatments to facilitate fibrillation during HPH. Two types of mechanical techniques were tested: disintegration (D) and milling (M). Additionally, some samples were dried (S). Table 4.1 shows OM images of the cellulose fibres according to the pre-treatment or combinations of pre-treatments applied.

When the raw materials are D, bundles of cellulose fibres are clearly observed. However, they have large dimensions both in diameter and length. Since leek and lettuce rot within a week, it would be preferred to store them dried, ensuring longer conservation and facilitating their transportation. Therefore, the drying of the disintegrated samples (DS) was tested. The OM images of Table 4.1 show that DS promotes the agglomeration of the bundles of fibres. The same behaviour is observed after milling the DS sample (DSM) and when the raw materials are only milled and not disintegrated initially (SM). For SMD pre-treatment, the fibres are more individualized and have lower dimensions than D samples.

Table 4.1. OM images (5× magnification) of pre-treated cellulose fibres.

	D	DS	DSM	SM	SMD
Leek	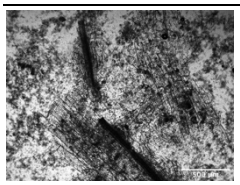	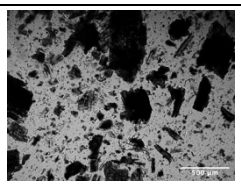	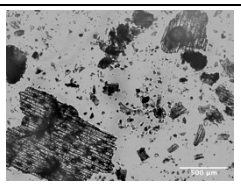	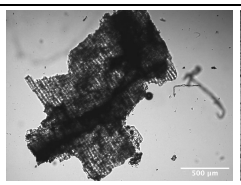	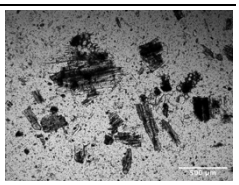
Lettuce	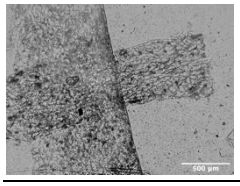	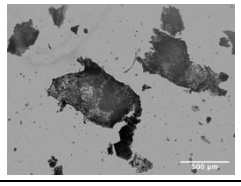	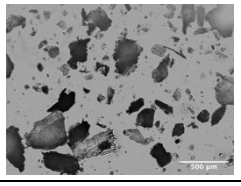	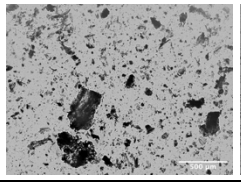	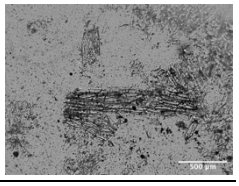

(D) desintegrated; (DS) desintegrated + dried; (DSM) desintegrated + dried + milled; (SM) dried + milled; (SMD) dried + milled + desintegrated

DS, DSM, and SM combinations of pre-treatments do not satisfy their purpose of facilitating fibre separation. Therefore, they are considered inadequate for the performance of the next step, HPH. According to OM results in Table 4.1, the best pre-treatments are D and SMD. Thus, 1 pass of HPH was tested for leek and lettuce after they were submitted to D and SMD combinations of pre-treatments.

Nevertheless, the D leek and lettuce pulps had homogenization problems. The equipment clogged several times due to the large dimensions of cellulose fibres (as observed in the OM images of Table 4.1). Therefore, the treatment could only be performed after the dilution of the samples. On the other hand, SMD pulps passed with no equipment difficulties. Table 4.2 shows the OM images of the leek and lettuce pulps after D and SMD pre-treatments before and after 1 pass of HPH.

Table 4.2. Mechanical pre-treatment selection: consistency, transmittance (600 nm), and OM images (5× magnification).

	Leek | 600 bar			
Parameter	**D-HPH-0-Leek**	**D-HPH-1-Leek**	**SMD-HPH-0-Leek**	**SMD-HPH-1-Leek**
Consistency / wt.%	4.03 ± 0.07	1.47 ± 0.04	4.75 ± 0.02	3.91 ± 0.13
Transmittance 600 nm / %	30.1 ± 0.1	17.5 ± 0.2	18.5 ± 0.3	11.5 ± 0.1
Optical Microscopy	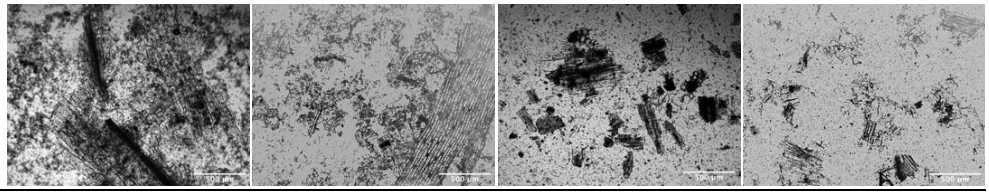			
	Lettuce | 600 bar			
Parameter	**D-HPH-0-Lettuce**	**D-HPH-1-Lettuce**	**SMD-HPH-0-Lettuce**	**SMD-HPH-1-Lettuce**
Consistency / wt.%	3.60 ± 0.07	1.22 ± 0.01	4.54 ± 0.07	3.58 ± 0.09
Transmittance 600 nm / %	24.5 ± 0.1	14.8 ± 0.1	16.5 ± 0.1	11.2 ± 0.1
Optical Microscopy	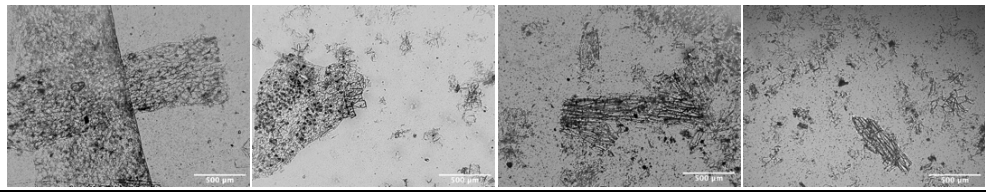			

(D) desintegrated; (SMD) dried + milled + desintegrated; (HPH) high-pressure homogenization; (0,1) number of HPH passe

The consistencies of D-HPH-1-Leek and -Lettuce (1.47 and 1.22 wt.%, respectively) presented in Table 4.2 correspond to the maximum values that can be attained for samples with D pre-treatment after HPH. In contrast, SMD-HPH-1-Leek and -Lettuce were homogenized with more than twice the consistency (3.91 and 3.58 wt.%, respectively). Since HPH requires high energy consumption to operate, it is preferred to treat suspensions at higher consistencies, i.e., with more cellulose fibres in the same amount of sample, to make the treatment more economically viable.

OM images of Table 4.2 show that 1 pass of HPH did not produce fibres with a homogeneous diameter for either pre-treatment since a broad dimension range of fibres is visualised. However, while D samples have bundles of fibres with a diameter up to 580 μm (leek) or 840 μm (lettuce), in SMD samples, the larger fibres have diameters of 200 μm (leek) or 500 μm (lettuce), measured from the larger fibres observed in the OM images. Thus, SMD pre-treatment enables a narrower particle size distribution that will produce emulsions with higher stability according to the studies of Lu et al. (2020). Therefore, the mechanical pre-treatment selected was SMD for both leek and lettuce.

4.2 Characterization of the raw materials and cellulose fibres

In the second phase of this work, the solids content of leek and lettuce and their chemical composition were determined. Additionally, throughout HPH, consistency was obtained, and fibrillation was monitored by morphological characterization.

4.2.1 Compositional characterization of raw materials

Drying of the leek and lettuce food waste enabled the determination of their solids content, as shown in Table 4.3. The solids content includes not only cellulose, but also ash, extractives, pectin, hemicellulose, and lignin composition of the raw materials.

Table 4.4 shows the chemical composition of the solids content of the raw materials and the centrifugated lettuce. As observed, the cellulose composition of leek, lettuce, and centrifugated lettuce is within a range of 14-25 wt.%. Sanchez-Salvador et al. (2019) reported the production of Pickering emulsions containing cellulose from cotton, which is 99.9 wt.% composed of cellulose. The extraction of the additional components from the raw materials would imply undesirable chemical treatments for food-grade products application. On the other hand, Lu et al. (2020) reported the production of Pickering emulsions with apple pomace that, similarly to leek and lettuce, has a cellulose composition of 17.7 wt.% (Ma et al., 2019). Thus, cellulose was not isolated from leek and lettuce pulps.

Table 4.3. Solids content of the raw materials.

Raw material	Solids content / wt.%
Leek	11.2 ± 1.5
Lettuce	5.3 ± 0.1

Table 4.4. Solids content characterization of leek, lettuce, and centrifugated lettuce pulps after drying and milling.

	Leek	Lettuce	Centrifugated Lettuce
Ash / wt.%	10.8 ± 0.1	27.1 ± 0.4	14.9 ± 0.5
Extractives / wt.%	9.2 ± 0.7	14.4 ± 0.9	10.9 ± 1.0
Pectin / wt.%	16.2 ± 0.3	12.9 ± 0.3	16.0 ± 0.3
Cellulose / wt.%	25.8 ± 0.6	14.3 ± 0.3	19.8 ± 0.2
Hemicellulose / wt.%	12.7 ± 0.3	6.1 ± 0.2	6.8 ± 0.1
Soluble Lignin / wt.%	20.5 ± 0.7	20.0 ± 0.4	20.7 ± 0.5
Insoluble Lignin / wt.%	4.9 ± 0.4	5.2 ± 0.4	11.0 ± 0.1

In order to reduce the HPH energy consumption, charged groups are typically introduced into the cellulose fibres by a chemical pre-treatment, such as TEMPO-mediated oxidation, which replaces hydroxyl groups with carboxylic groups. The electrostatic repulsion effect between charges promotes fibrillation during the mechanical treatment. As Table 4.5 shows, leek and lettuce are naturally composed of carboxylic groups, so their addition by chemical treatment was unnecessary.

Table 4.5. Carboxylic groups composition of leek and lettuce.

Raw material	Carboxylic Groups / mmol COOH g^{-1}
Leek	0.72 ± 0.05
Lettuce	2.67 ± 0.04

4.2.2 Consistency throughout HPH

Consistency was calculated after 1 pass, to determine its maximum attainable value after HPH, and throughout HPH, to monitor the dilution of the pulps. Leek (HPH-9-LC-Leek) and lettuce (HPH-9-LC-Lettuce) were first homogenized at low consistency. A second attempt for high consistencies was performed for both raw materials. As shown in Table 4.6, Leek (HPH-9-HC-Leek) was able to pass at a higher consistency (5.28 instead of 3.91 wt.%). Lettuce was only able to pass at low consistency (~3.5 wt.% for both tests). After centrifugation, the pellet used in C-HPH-1-Lettuce had high consistency and had to be properly diluted before HPH, which resulted in a very low consistency after 1 pass (1.93 wt.%).

In all homogenization sequences, the minimum amount of water was added during the first pass to ensure that the equipment operated without clogging. Thus, in SMD pre-treatment, the highest consistencies that enable HPH correspond to those of HPH-9-HC-Leek for leek, HPH-9-LC-Lettuce for lettuce, and C-HPH-1-Letuce for centrifugated lettuce.

Table 4.6. Pulp consistency evolution throughout HPH.

	Consistency / wt.%				
Passes of HPH	**0**	**1**	**3**	**6**	**9**
HPH-9-LC-Leek	4.75 ± 0.02	3.91 ± 0.13	3.65 ± 0.11	3.64 ± 0.01	3.74 ± 0.01
HPH-9-HC-Leek	7.54 ± 0.15	5.28 ± 0.04	5.47 ± 0.01	5.44 ± 0.05	5.46 ± 0.02
HPH-9-LC-Lettuce	4.54 ± 0.09	3.58 ± 0.09	3.19 ± 0.21	3.21 ± 0.02	3.38 ± 0.03
C-HPH-1-Lettuce	5.79 ± 0.05	1.93 ± 0.03	-	-	-

(HPH) High-pressure homogenization; (1, 9) number of HPH passes; (LC) Low consistency; (HC) High consistency

4.2.3 Morphological characterization

Increasing HPH passes should enable the separation of the microfibres from the main fibre structure, resulting in ramified fibres or individual microfibres, if they can completely separate from the main fibre. In addition, HPH also reduces the fibres' diameter. Thus, a homogeneous size distribution should be achieved after several HPH passes (Sanchez-Salvador et al., 2021).

As observed from the OM images throughout HPH of Table 4.7, no raw material attained a homogeneous nano size distribution after 9 passes. Instead, bundles of microfibres are still observed. However, there is a clear diameter and length reduction after HPH, which is more evident at the first pass. From 6 to 9 passes, there are no evident changes in morphology as observed by OM images. For those passes, HPH-9-LC-Lettuce fibres are almost completely ramified contrarily to HPH-9-LC-Leek and HPH-9-HC-Leek, where many structures with longer diameters and lengths are still observed. Lettuce has higher carboxylic groups content than leek, as shown in Table 4.5, which is expected to promote better fibrillation.

Table 4.7. Optical microscopy images (5× magnification) of the different homogenization sequences throughout HPH.

	passes of HPH				
	0	**1**	**3**	**6**	**9**
HPH-9-LC-Leek	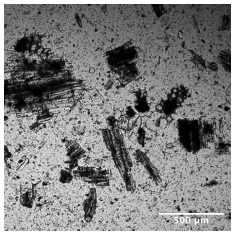	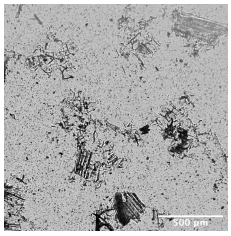	-	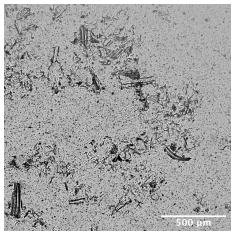	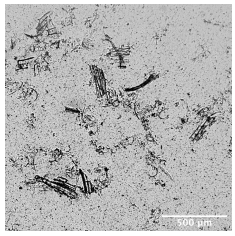
HPH-9-HC-Leek	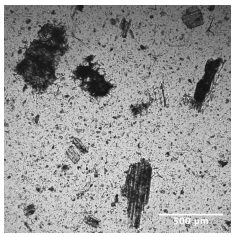	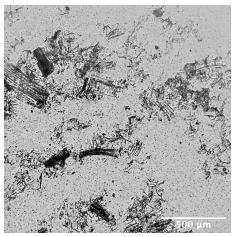	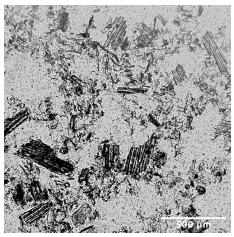	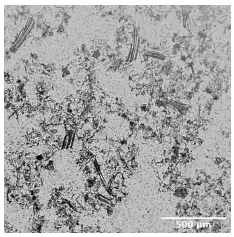	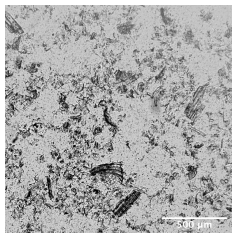
HPH-9-LC-Lettuce	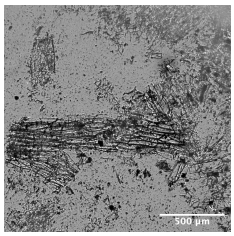	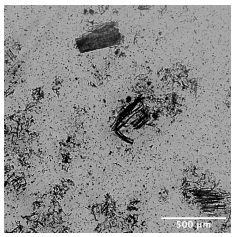	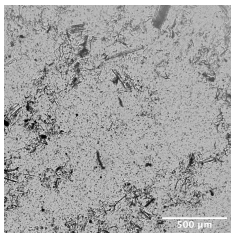	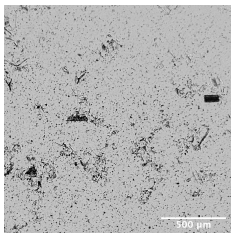	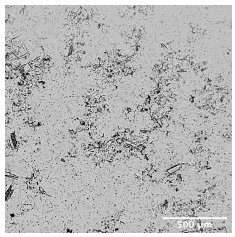
C-1-HPH-Lettuce	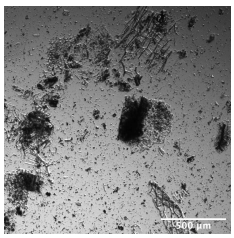	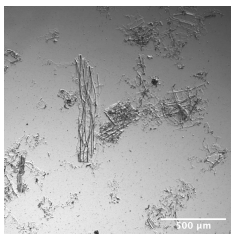	-	-	-

(HPH) high-pressure homogenization; (1,9) number of HPH passes; (LC) low consistency; (HC) high consistency; (C) centrifugated

In addition to OM analysis, fibrillation throughout HPH was monitored through the determination of the aspect ratio (AR), polymerization degree (PD), transmittance at 600 nm, and cationic demand (CD). Figure 4.1 shows the results obtained.

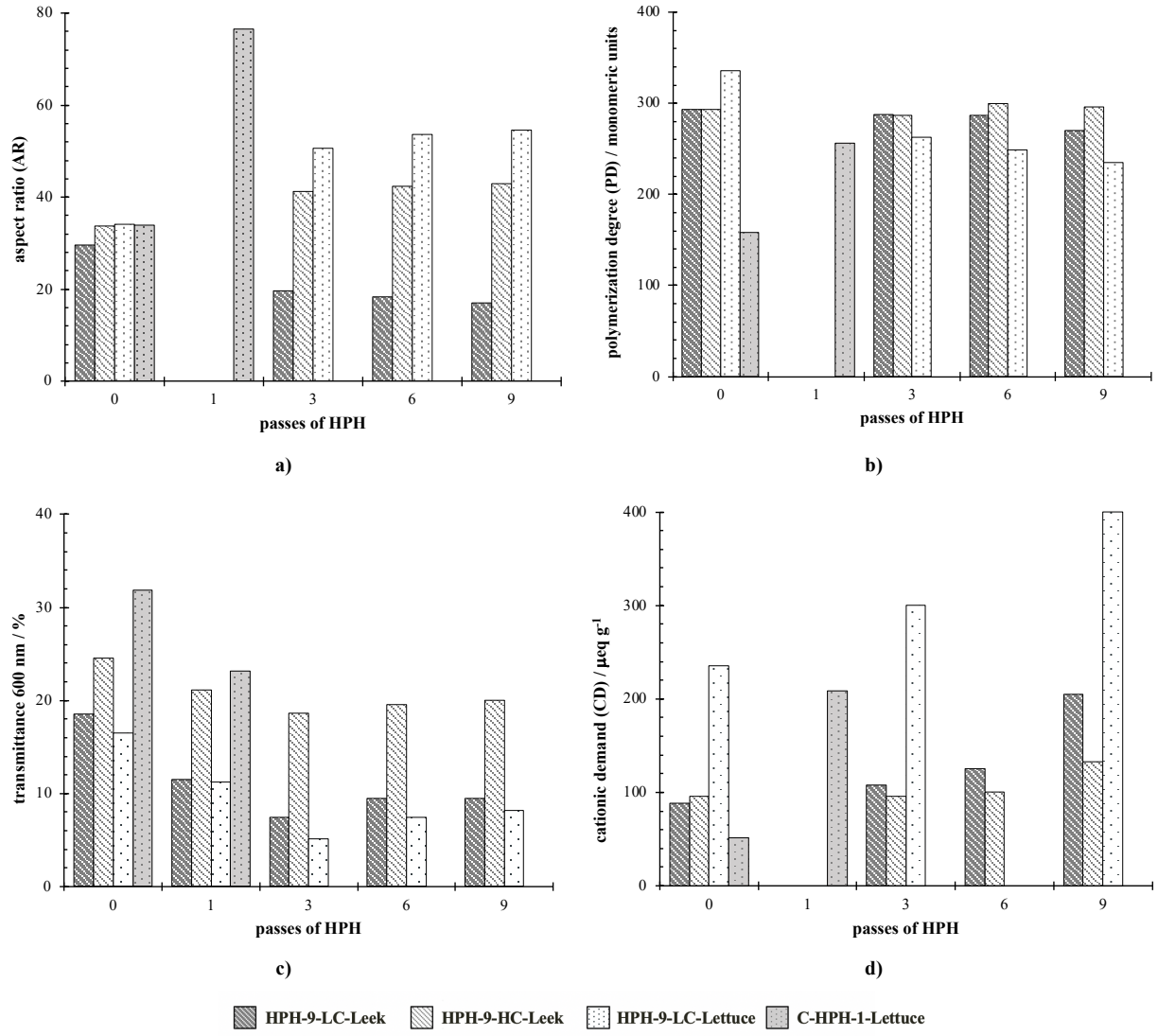

Figure 4.1. Evolution of a) aspect ratio (AR); b) polymerization degree (PD); c) transmittance at 600 nm; d) cationic demand (CD), throughout HPH.

The same combination of pre-treatments resulted in an initial AR (Figure 4.1a)) similar for both raw materials, which is approximately 30, independently of the homogenization sequence. After 3 passes of HPH for HPH-9-HC-Leek and HPH-9-LC-Lettuce, and 1 pass for C-HPH-1-Lettuce, an increase in AR was observed from the reduction in fibres diameter during the mechanical treatment. In contrast, AR of HPH-9-LC-Leek decreased after 3 passes of HPH. During the mechanical treatment, both diameter and length are reduced. Thus, in this case, the diameter reduction was inferior to the shortening of the cellulose fibres within the first 3 passes. After 3 passes, AR remained almost constant for all the homogenization sequences analysed, which is consistent with the OM images of Table 4.7 that do not show significant differences in fibres' size. In addition, as observed from OM images, the fibres' separation is more significant in lettuce than in leek, thus there is a higher AR for the first raw material.

PD also highlights better fibrillation for lettuce. The mechanical treatment reduces the number of anhydroglucose units significatively to obtain CNF. Thus, as Figure 4.1b) shows, PD is lower in lettuce than in leek after HPH. Moreover, and as already observed by OM analysis and from AR, there are no significant changes in PD after 3 passes, i.e., there is low fibre's breakage during HPH.

Transmittance at 600 nm (Figure 4.1c)) was used as an indicator of the nanofibres content. When fibres have large dimensions or are in bundles, the light beam is scattered or diffracted, and the particles show lower transmittance. On the other hand, when particles have dimensions in the nanometre range, they are too small to scatter much light, becoming optically transparent, i.e., with transmittance approaching 100 % (Nakatani & Sato, 2017). For samples with impurities that absorb light, transmittance has lower values and never reaches 100 % for maximum fibrillation (Balea, 2017).

As Figure 4.1c) shows, no sample has transmittance values above 35 %, indicating the existence not only of fibres with dimensions over the nanometre range, but also of compounds besides cellulose (Table 4.4). The presence of bundles of fibres is identified from the transmittance values. There is an initial decrease in transmittance, between 0 and 3 passes, which corresponds to the separation of the original bundles of fibres into bundles of smaller dimensions that are still able to absorb light. From 3 to 6 passes there is a slight increase in transmittance from the existence of more particles with smaller dimensions, which do not absorb light. Lettuce (HPH-9-LC-Lettuce) shows lower transmittance since it is composed of more impurities than leek (HPH-9-LC-Leek and -HC-Leek) (Table 4.4). In contrast, when lettuce is centrifugated (C-HPH-1-Lettuce) and some of the impurities are removed, higher transmittance is obtained.

CD, which measurements are made at surface, increases throughout HPH. The separation of fibres from the bundles implies more hydroxyl groups with a negative charge at surface. Lettuce and leek pulps are typically anionic due to the presence of negatively charged carboxylic groups (Table 4.5). According to Figure 4.1d), lettuce (HPH-9-LC-Lettuce) has higher CD than leek (HPH-9-LC-Leek and -HC-Leek), due to lettuce's higher composition in carboxylic groups (2.67 versus 0.72 mmol COOH g^{-1}, respectively). Centrifugated lettuce (C-HPH-1-Lettuce) carboxylic groups content was not measured. However, CD before HPH indicates that it is lower than leek and lettuce's.

4.3 Conditions of cellulose fibres production for Pickering emulsions application

As described in Chapter 3, preliminary studies were made to evaluate the potential of cellulose fibres previously produced from leek and lettuce agricultural residues as Pickering emulsions stabilizers. According to stability after 48 h, the best homogenization sequence and the respective optimal number of HPH passes were evaluated for each raw material.

4.3.1 Leek

For leek, Pickering emulsions were produced at fixed O/W ratio of 40/60 wt.% and pulp's solid content in the aqueous phase (PSC) of 2.25 wt.%. The emulsion, oil, and water phase distribution and respective emulsifying index (EI) after 48 h are shown in Figure 4.2. As observed, an emulsion phase after 48 h is observed in all formulations. This is the first proof that leek cellulose fibres act as Pickering stabilizers.

An aqueous layer was formed bellow the emulsion phase for all samples tested. Additionally, in some of the emulsions (0 and 9 HPH passes for HPH-9-LC-Leek; 0 and 3 HPH passes for HPH-9-HC-Leek), an oil layer was formed on top of the emulsion phase. This indicated that, even at the highest degree of fibrillation tested, there was not a completely stable emulsion, i.e., with $EI = 100$ wt.%, for a formulation of 40/60 wt.% O/W ratio and 2.25 wt.% PSC. However, $EI > 95$ wt.% is a promising stability result.

For HPH-9-LC-Leek, EI increased from 0 to 6 HPH passes. From 6 to 9 passes, there was no significant change. For HPH-9-HC-Leek, a similar tendency was observed, with the EI increasing significantly from 0 to 6 HPH passes and not changing much from 6 to 9 passes.

Thus, results from both homogenization sequences indicated that the higher energy demand involved in performing 9 passes instead of 6 would not provide substantial advantages for Pickering emulsion stabilization. Therefore, 6 were considered as the optimal number of HPH passes.

EI at 6 passes of HPH-9-HC-Leek was considerably higher than HPH-9-LC-Leek. HPH-9-HC-Leek also had the advantage of having higher consistency than HPH-9-LC-Leek, having spent less energy to homogenize the same initial amount of raw material. Therefore, HPH-9-HC-Leek was selected for the following stability study.

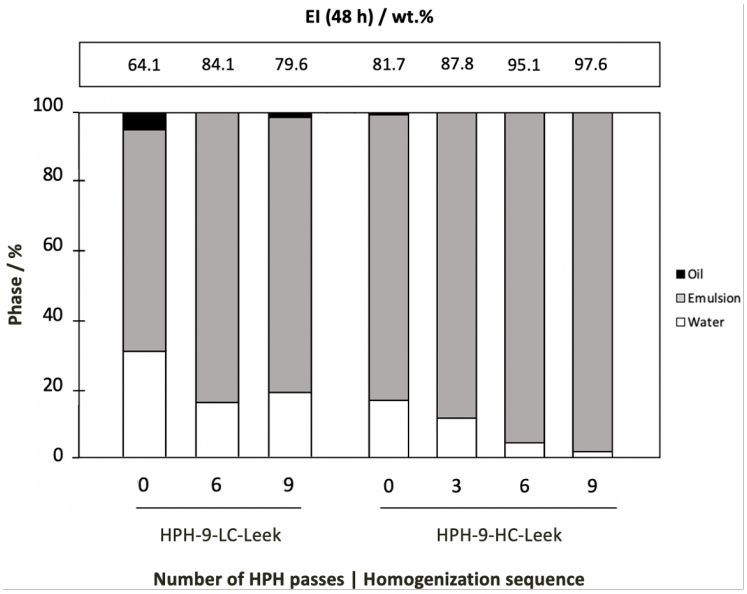

Figure 4.2. Phase distribution and EI after 48 h of Pickering emulsions produced with HPH-9-LC-Leek and HPH-9-HC-Leek pulps (40/60 wt.% O/W ratio; 2.25 wt.% PSC).

4.3.2 Lettuce

For lettuce, Pickering emulsions were produced at fixed O/W ratio of 40/60 wt.%. Due to C-HPH-1-Lettuce consistency after the first pass of HPH, 1.93 wt.% (Table 4.6), PSC had to be fixed at a lower value than leek, 1.0 wt.%. Figure 4.3 shows emulsion, oil, and water phase distribution and the respective EI after 48 h. An emulsion phase after 48 h is visible in all samples prepared with lettuce pulp containing cellulose fibres, meaning it can successfully act as a stabilizer in Pickering emulsions.

At O/W ratio of 40/60 wt.% and PSC of 1.0 wt.%, the formation of aqueous and oil layers can be observed in all emulsions produced. Thus, this is not considered a stable formulation.

In HPH-9-LC-Lettuce, EI decreased from 0 to 9 HPH passes, an opposite behaviour to the one observed for leek. Therefore, according to these results, lettuce fibres enable better stability when they are in bundles of fibres of large dimensions.

C-HPH-1-Lettuce was performed to evaluate the stability of lettuce after centrifugation. According to Table 4.4, the removal of the supernatant reduced the ash and extractives content in the pulp to values closer to the leek. As a result, C-HPH-1-Lettuce showed higher EI than HPH-9-LC-Lettuce at 0 passes, proving centrifugation to be advantageable. After 1 pass of HPH, similar stability was reported. Thus, C-HPH-1-Lettuce with 0 passes of HPH was selected for the following study.

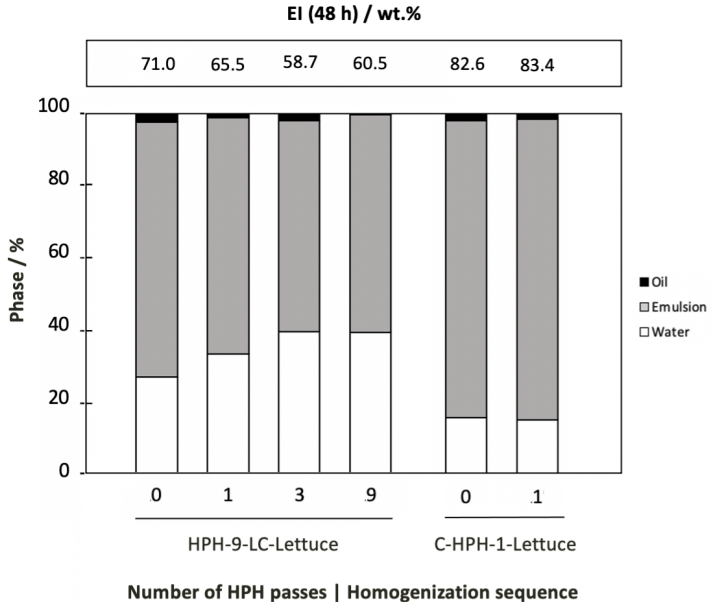

Figure 4.3. Phase distribution and EI after 48 h of Pickering emulsions produced with HPH-9-LC-Lettuce and C-HPH-1-Lettuce pulps (40/60 wt.% O/W ratio; 1.0 wt.% PSC).

4.3.3 SEM and diameter distribution of cellulose fibres for Pickering emulsions application

For the selected leek and lettuce pulps, the morphology of the cellulose fibres was observed from SEM images and the fibres size distribution, in terms of number and volume, from laser diffraction analysis as shown in Table 4.8.

The fibre diameter distribution versus the number of fibres shows that most leek fibres are in the nano range, with an average diameter of (83 ± 1) nm. In contrast, lettuce, which did not go through HPH, has an average diameter in the micrometre range, (0.7 ± 0.2) µm, and does not contain appreciable nanofibres.

The particle diameter distribution versus volume of particles evidences the heterogeneous size distribution of the fibres. For both raw materials, most of the pulp's volume is occupied by particles of much larger diameter than the average mentioned above: (41 ± 1) µm for leek and (259 ± 7) µm for lettuce. These correspond to the bundles of fibres seen in OM images (Table 4.7) that are also visible in SEM images.

Even though the leek pulp contains fibres with nanometre diameters, the cellulose fibres present in both pulps will be identified as CMF since most of the volume is occupied by particles with the characteristic dimension within the micrometre range.

Table 4.8. Leek and lettuce SEM images and fibre diameter distribution in terms of a) number and b) volume.

	SEM images	fibres diameter distribution	
		a)	b)
HPH-9-HC-Leek | 6 passes	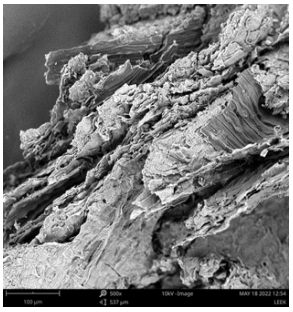	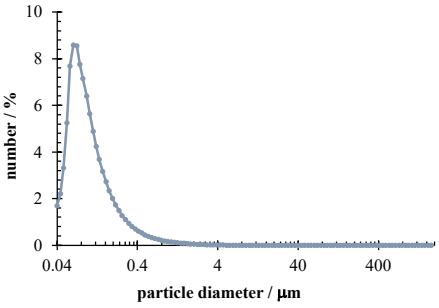	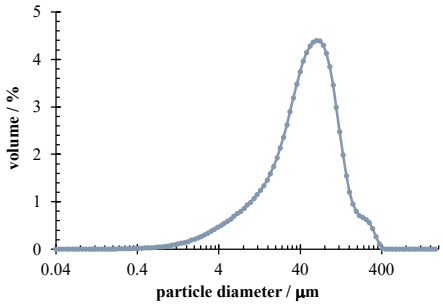
C-HPH-1-Lettuce | 0 passes	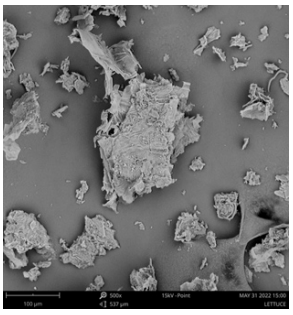	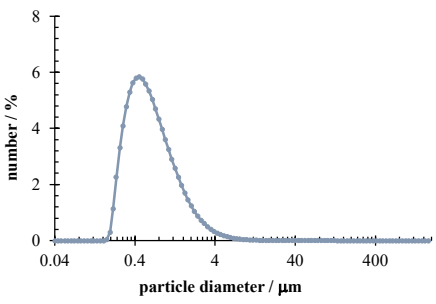	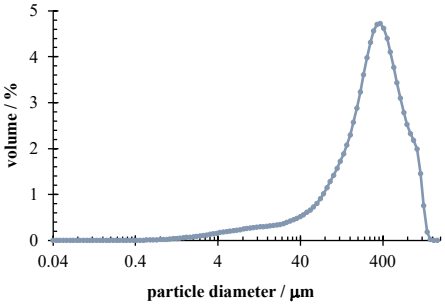

4.4 Pickering emulsions

Pickering emulsions were prepared at different O/W ratios and PSC using the leek and lettuce pulps selected in Section 4.3. The emulsion type was evaluated for all formulations as well as their stability after 48 h. Additionally, OM and CLSM images enabled the observation of the fibres' stabilization mechanism of the O/W interface and the determination of the dispersed phase droplet size distribution. Finally, rheological studies were performed.

4.4.1 Rotor-stator homogenizer conditions

Before the stability studies at different O/W ratios and PSC, the optimal conditions of operation of the rotor-stator homogenizer used during emulsification were evaluated. Thus, Pickering emulsions with the same

O/W ratio (40/60 wt.%) and PSC (3.0 wt.%) were prepared at different t_{stirring} and rotor-stator speeds. Leek pulp was used for these tests. Table 4.9 shows t_{stirring} and ΔT during the emulsification process. Figure 4.4 shows the distribution of the oil, water, and emulsion phases after 48 h and the respective EI.

According to the results of Table 4.9, C4 conditions enabled ΔT of only 1 °C. It was important to avoid emulsification at high temperatures since emulsions' properties can be changed and the natural CMF can be damaged. For this experiment, the mixing speed considered corresponded to the lowest available in the rotor-stator homogenizer used; $t_{\text{stirring}} = 26$ s was the necessary time to obtain a homogeneous emulsion phase. Although the EI (Figure 4.4) is very similar for all experiments, C4 reported the highest value. Thus, the rotor-stator homogenizer speed was fixed at 11 000 rpm and t_{stirring} at $t_{\text{injection}}$

Table 4.9. Rotor-stator homogenizer conditions (leek CMF; 40/60 wt.% O/W ratio; 3.0 wt.% PSC): time of stirring and variation of temperature between dispersion and stirring.

Experiment	Speed / rpm	t_{stirring}	ΔT / °C
C1	16 000	3 min	9
C2	16 000	24 s	4
C3	11 000	3 min	5
C4	11 000	26 s	1

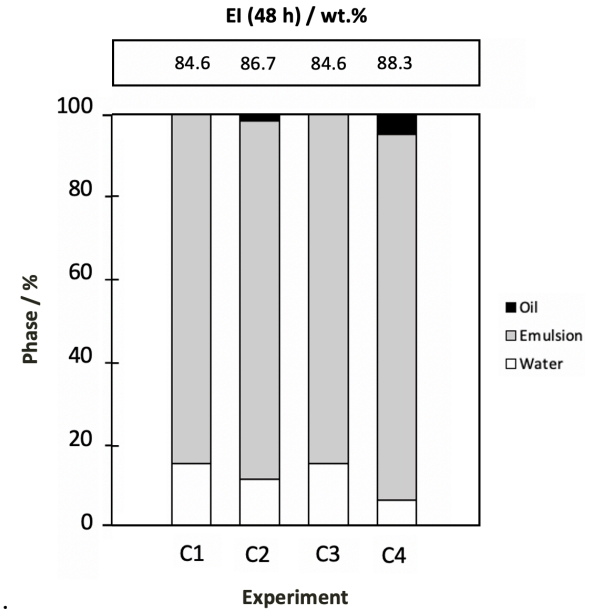

Figure 4.4. Rotor-stator homogenizer conditions (leek CMF; 40/60 wt.% O/W ratio; 3.0 wt.% PSC): phase distribution and EI after 48 h.

An additional study on particle size dependence on $t_{\text{dispersion}}$ and rotor-stator homogenizer speed, described in Appendix A, showed that agitation time and rotation speed of the rotor-stator homogenizer do not influence the size distribution of leek CMF. Thus, $t_{\text{dispersion}}$ was fixed at 1 min just to ensure appropriate dispersion of the fibres in water.

4.4.2 Pickering emulsions type

Pickering emulsions type was first predicted before the emulsion's production by determining the contact angle measured through the water phase (θ) of leek and lettuce fibres. Table 4.10 shows the results obtained. Lu et al. (2020) reports that θ decreases as the particle diameter of fibres from apple pomace decreases. This occurs because when the fibre size is smaller, more hydroxyl groups are exposed on the surface, making the particles more hydrophilic, i.e., with smaller θ. However, this direct comparison between particle size cannot be made for leek and centrifugated lettuce since they have different compositions and an heterogenous size distribution. As observed in Table 4.10, both raw materials have similar θ of values $< 90°$, i.e., they have hydrophilic affinity and thus they are expected to stabilize oil-in-water emulsions.

Table 4.10. Contact angles measured through the water phase of leek and lettuce.

Leek	Lettuce
	
72.8 ± 4.8	71.9 ± 1.8

Emulsion type was confirmed from drop test after the emulsion's production. For all formulations, it was observed that drops only dispersed in the water phase, which is characteristic of an oil-in-water Pickering emulsion. Figure 4.5 shows a representative image of the registered behaviour.

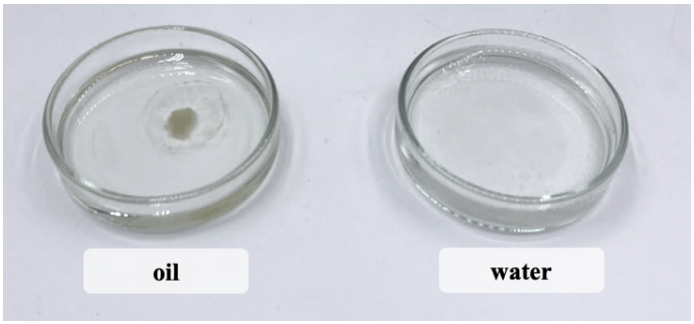

Figure 4.5. Drop test in oil and water: leek CMF, 40/60 wt.% O/W ratio, and 1.0 wt.% PSC.

4.4.3 Stability tests for Pickering emulsions containing leek CMF

According to the studies of Sanchez-Salvador et al. (2019) and Lu et al. (2020), the increase of mass fraction of CMF in the aqueous phase resulted in the increase of the emulsion phase. Since the CMF used to produce the Pickering emulsions in this study was in pulp form, there was a limiting consistency in the aqueous phase to each O/W ratio. Thus, an initial stability study at maximum leek PSC was performed, considering different O/W ratios. Figure 4.6 shows emulsion, oil, and water phase distribution and the corresponding EI 48 h after emulsification.

The increase of oil content in the emulsion implies the formation of more droplets and the consequent need of CMF to stabilize it. As Figure 4.6 shows**,** the maximum PSC decreased as the O/W ratio increased, which resulted in less available CMF. Therefore, an oil layer larger in volume for higher O/W ratios is formed on top of the emulsion phase. Meanwhile, EI decreased for emulsions with a higher amount of oil.

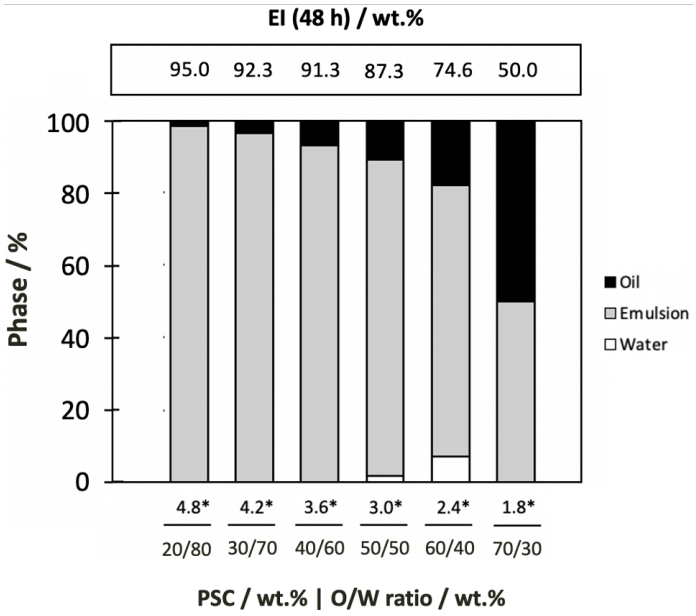

Figure 4.6. Phase distribution and EI after 48 h of Pickering emulsions containing leek CMF at maximum (*) PSC.

According to the results of Figure 4.6, a second set of formulations was prepared. The O/W ratios with EI > 90 wt.% (20/80, 30/70, and 40/60 wt.%) were considered for a stability study varying the PSC. The goal was to determine if a stable formulation was obtained using less raw material. Better stability was not expected since the oil layer on top indicated the need of more CMF.

Figure 4.7 shows the emulsion, oil, and water phase distribution 48 h after emulsification and the corresponding EI obtained. Stability results are in agreement with the studies of Sanchez-Salvador et al. (2019) and Lu et al. (2020), where it is reported that the increase of the emulsion phase is favoured by the increase of PSC. For 20/80 and 30/70 wt.% O/W ratios, two different formulations resulted in EI > 90 wt.%: the one at maximum PSC and the one below. For 40/60 wt.% O/W ratio, only the formulation at maximum PSC exhibited EI > 90 wt.%.

As observed by the distribution of phases, only emulsions at maximum PSC completely eliminated the aqueous phase on the bottom of the vial. Meanwhile, for all formulations, an oil layer was formed on the top, which indicates that the PSC seems to not be enough to stabilize the oil droplets, resulting in their coalescence. To avoid this, a higher amount of CMF would be required, which the limiting consistency of the pulp does not allow. The highest EI (95.0 wt.%) was obtained at 20/80 wt.% O/W ratio and 4.8 wt.% PSC, the maximum PSC tested.

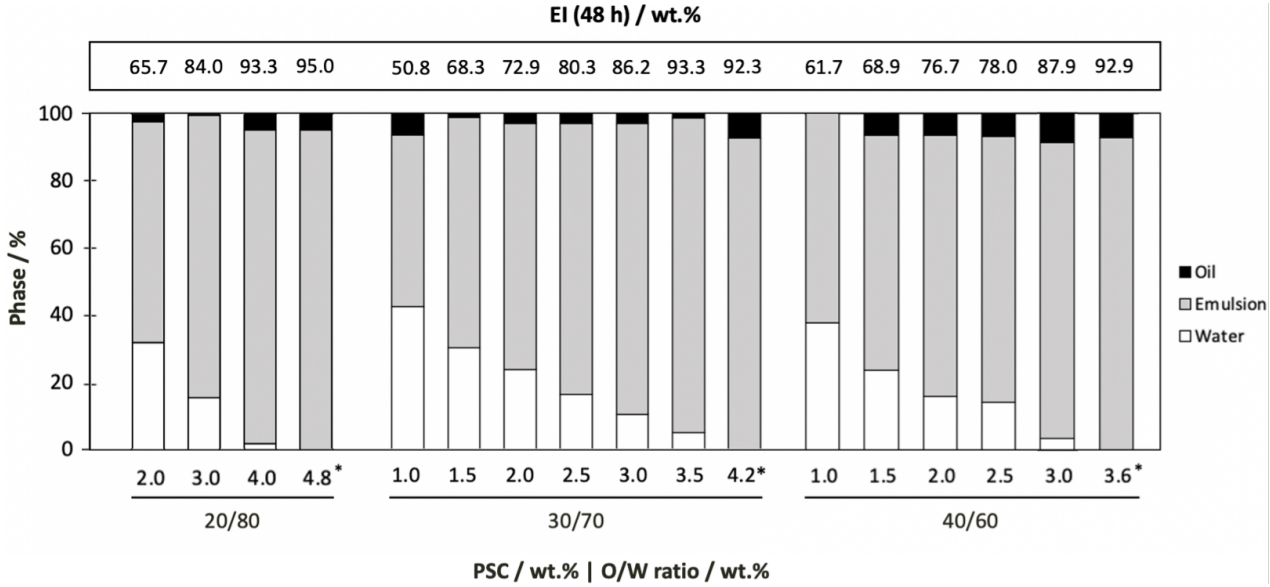

Figure 4.7. Phase distribution and EI after 48 h of Pickering emulsions containing leek CMF at different O/W ratios and PSC.

The stability results that were used to represent the phase distribution and to calculate the respective EI after 48 h (Figure 4.7) were obtained by visual inspection of the different formulations. Figure 4.8 shows the visual inspection results after 48 h of the emulsions containing leek CMF at maximum PSC for each O/W ratio, which were identified as the most stable formulations.

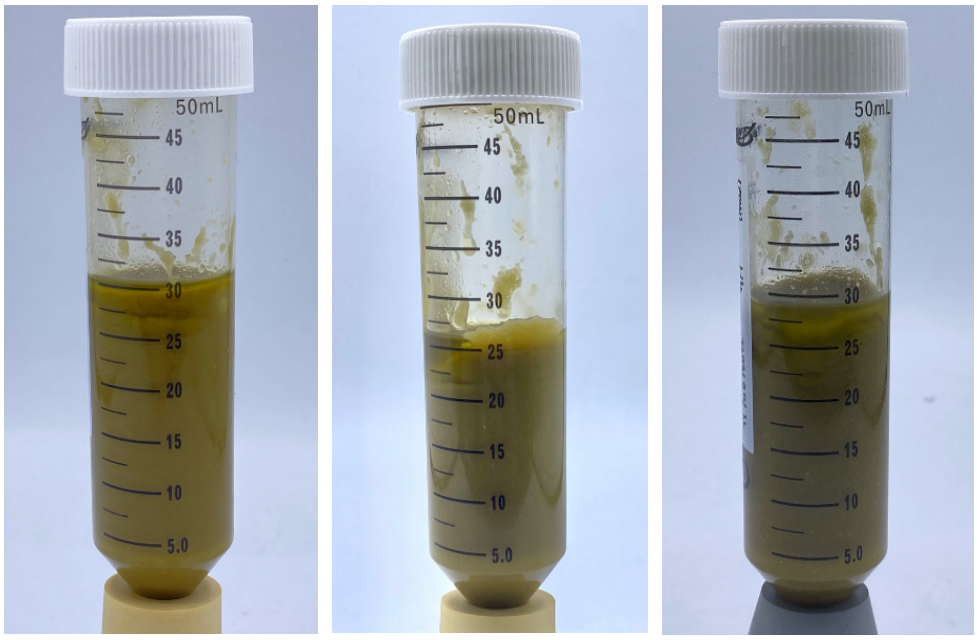

a) **b)** **c)**

Figure 4.8. Visual inspection after 48 h of Pickering emulsions containing leek CMF a) 20/80 wt.%, 4.8* wt.%; b) 30/70 wt.%, 4.2* wt.%; c) 40/60 wt.%, 3.6* wt.%.

4.4.4 Stability tests for Pickering emulsions containing lettuce CMF

Emulsion stability using lettuce pulp was also determined for the same O/W ratios considered for leek after the study at maximum PSC (20/80, 30/70, and 40/60 wt.%). Figure 4.9 represents the phase distribution

after 48 h and the corresponding EI. The phase distribution shows similar behaviour to leek's: for the three O/W ratios analysed, increasing the PSC raises the emulsion phase. As a result, higher EI is observed in samples with PSC of 3.8 wt.% (40/60 wt.% O/W ratio) and 4.0 wt.% (20/80 and 30/70 wt.% O/W ratios). Among these emulsions, the maximum EI (98.2 wt.%) is observed for 20/80 and 30/70 wt.% O/W ratios. For these formulations, corresponding to the most stable ones for each O/W ratio, the visual inspection results after 48 h are represented in Figure 4.10.

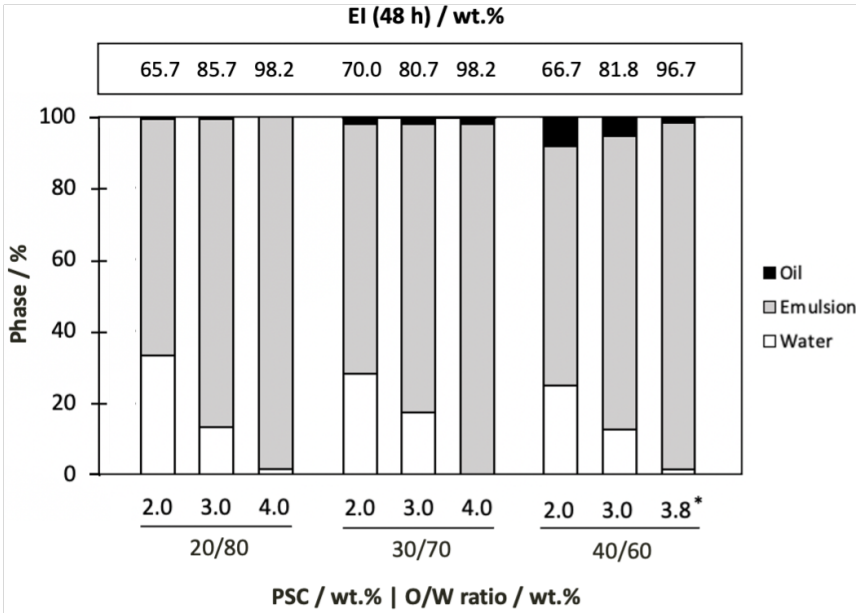

Figure 4.9. Phase distribution and EI after 48 h of Pickering emulsions containing lettuce CMF at different O/W ratios and PSC.

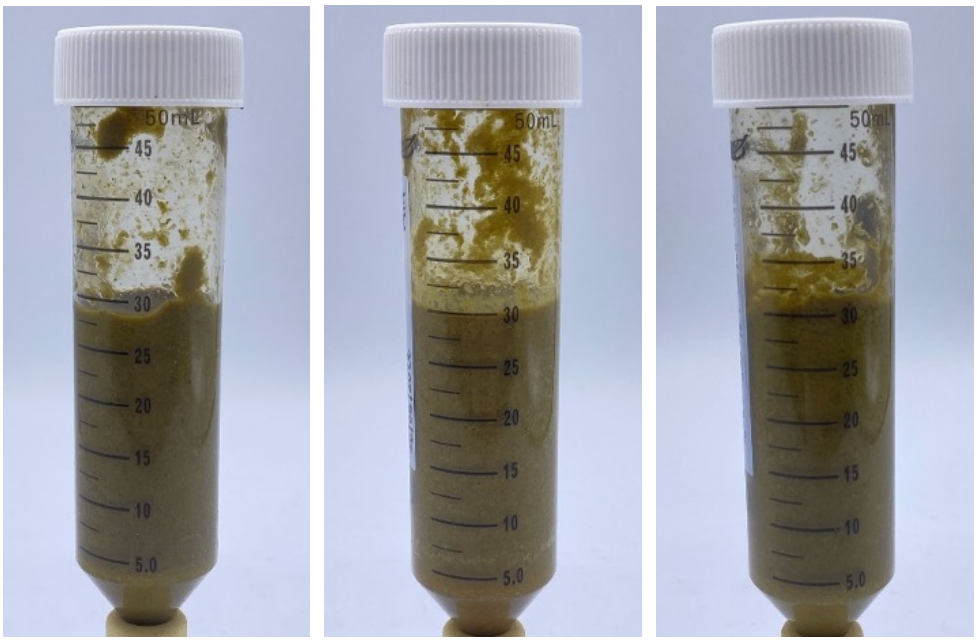

a) **b)** **c)**

Figure 4.10. Visual inspection after 48 h of Pickering emulsions containing lettuce CMF a) 20/80 wt.%, 4.0 wt.%; b) 30/70 wt.%, 4.0 wt.%; c) 40/60 wt.%, 3.8* wt.%.

4.4.5 Stabilization mechanism

The OM and CLSM images of Table 4.11 enable the observation of the oil droplets formed in Pickering emulsions. CLSM also shows the CMF's role at the O/W interface. These analyses were performed on Pickering emulsions at maximum leek PSC for different O/W ratios (20/80, 30/70, and 40/60 wt.%) and at 4.0 wt.% lettuce PSC and 30/70 wt.% O/W ratio. Due to the lack of stock of lettuce raw material, CLSM could only be performed for one formulation. Since the oil phase and CMF were stained with Nile Red and Blue, respectively, the green fluorescence in the images enables the identification of oil droplets, while the red fluorescence shows where fibres are located.

Table 4.11. OM (10× magnification) and CLSM images after emulsification of Pickering emulsions containing leek CMF a) 20/80 wt.%, 4.8* wt.%; b) 30/70 wt.%, 4.2* wt.%; c) 40/60 wt.%, 3.6* wt.%; and lettuce CMF d) 30/70 wt.%, 4.0 wt.%.

		OM images	CLSM images		
			oil droplets (Nile red 488 nm)	**CMF** (Nile blue 633 nm)	**oil droplets + CMF** (Nile red and Nile blue overlap)
a)	**Leek**	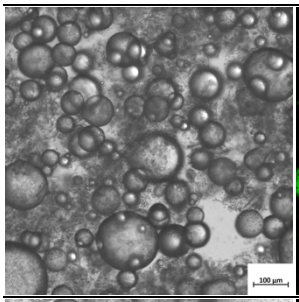	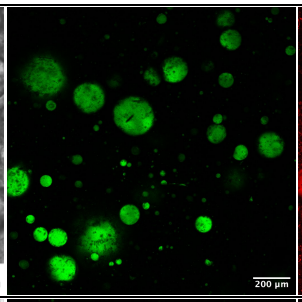	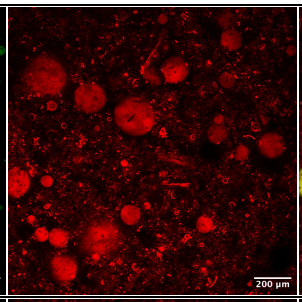	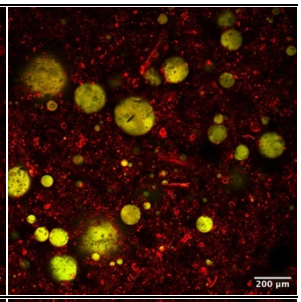
b)	**Leek**	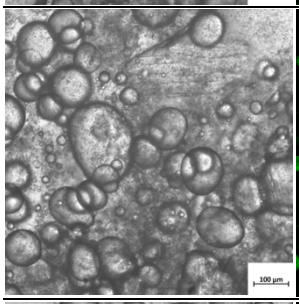	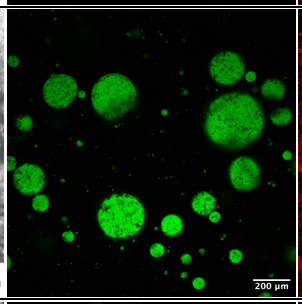	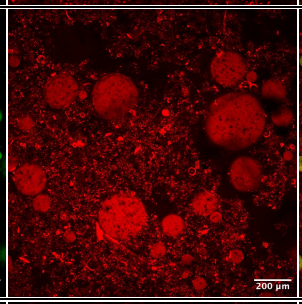	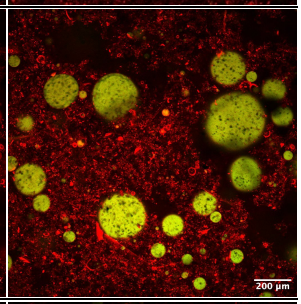
c)	**Leek**	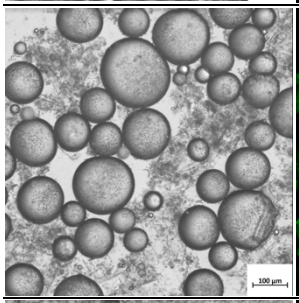	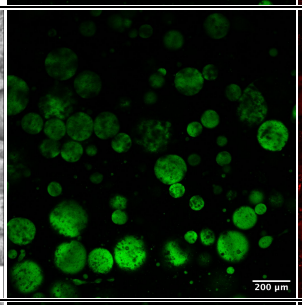	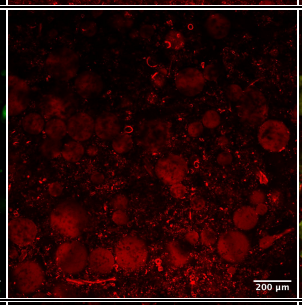	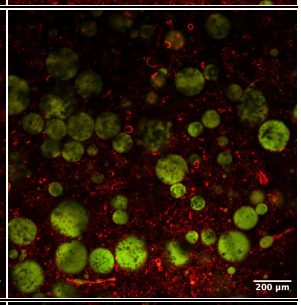
d)	**Lettuce**	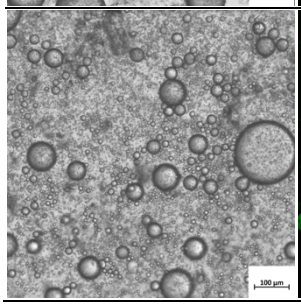	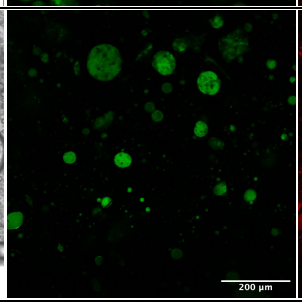	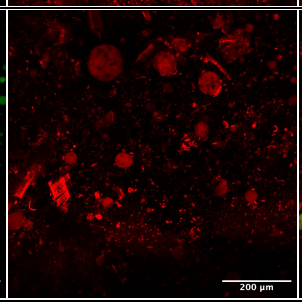	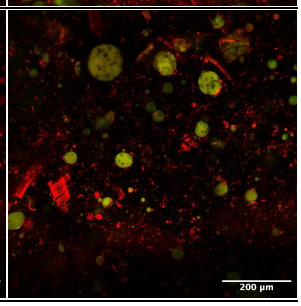

In both OM and CLSM images of Table 4.11 it is possible to identify bundles of cellulose fibres surrounding oil droplets of spherical shape and irregular size. These bundles enable the creation of a matrix around the oil droplets that covers all their surface, avoiding the droplets' coalescence. Due to the broad CMF diameter distribution (Table 4.8), the fibres are unevenly positioned, resulting in heterogeneous droplet sizes.

Typically, and as reported by Ribeiro et al. (2022) using nanohydroxyapatite and Lu et al. (2020) using apple pomace CMF, smaller oil droplets enable better stability results over time. In theory, for each shear rate applied by the rotor-stator, i.e., each rotor-stator speed, oil droplets of equal dimensions should be obtained, independently of the O/W ratio. Thus, variations in size are indicators of the coalescence of oil droplets when there are not enough solid particles available to completely cover the O/W interface of the smaller droplets.

In this work, considering the same rotor-stator speed of 11 000 rpm, larger oil droplets are observed in the OM and CLSM images using leek CMF, which indicates the coalescence of droplets. These results are according to the smaller stability shown by these leek CMF formulations (92.3 < EI < 95.0 wt.%) versus lettuce's (EI of 98.2 wt.%).

4.4.6 Rheological characterization

For each O/W ratio, rheological properties of the leek Pickering emulsions with the highest EI were analysed since they can influence to the emulsions' performance, appearance, and storage stability.

The relation of the viscosity (η) of the emulsions to the shear rate ($\dot{\gamma}$) in stationary state, represented in Figure 4.11, shows a viscosity decrease with the increase of shear rate, which indicates the non-Newtonian behaviour of the emulsions. However, for higher shear rates, the viscosity does not decrease so abruptly. The highest viscosity was achieved for 20/80 wt.% O/W ratio and 4.8 wt.% PSC.

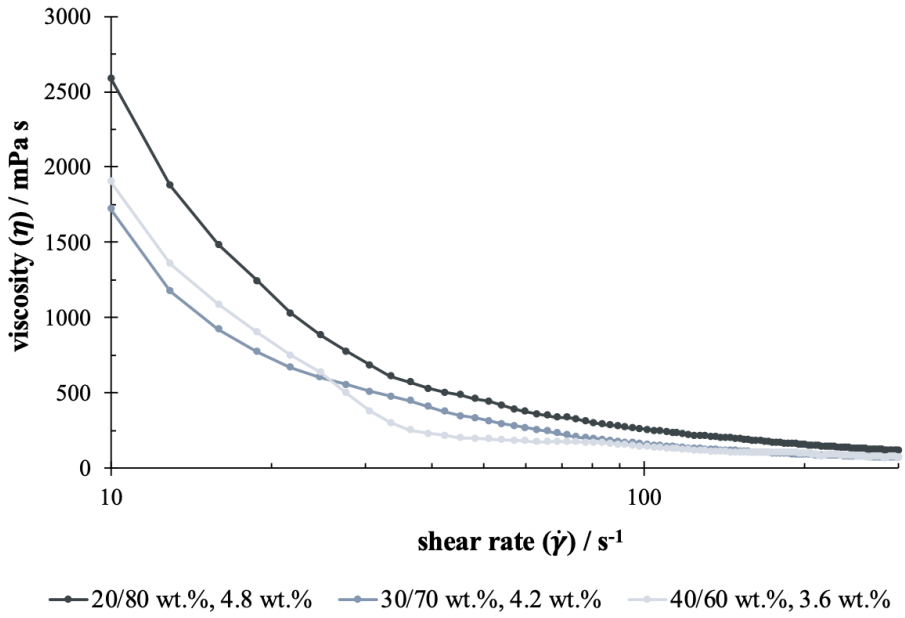

Figure 4.11. Viscosity of Pickering emulsions containing leek CMF at maximum PSC for different O/W ratios: viscosity (η) versus shear rate ($\dot{\gamma}$).

Pickering emulsions usually start to flow only after the applied stress exceeds a critical value, i.e., they have a yield stress. Below the yield stress, samples deform elastically, and above it, they deform permanently and flow like a liquid (*Understand Yield Stress Measurements*, 2015). Yield stress can be determined from the interception of the *yy* axis of the flow curve in Figure 4.12. Table 4.12 shows the corresponding yield stress values obtained. As observed, the highest yield stress (21 Pa) is reported for the formulation with highest EI after 48 h.

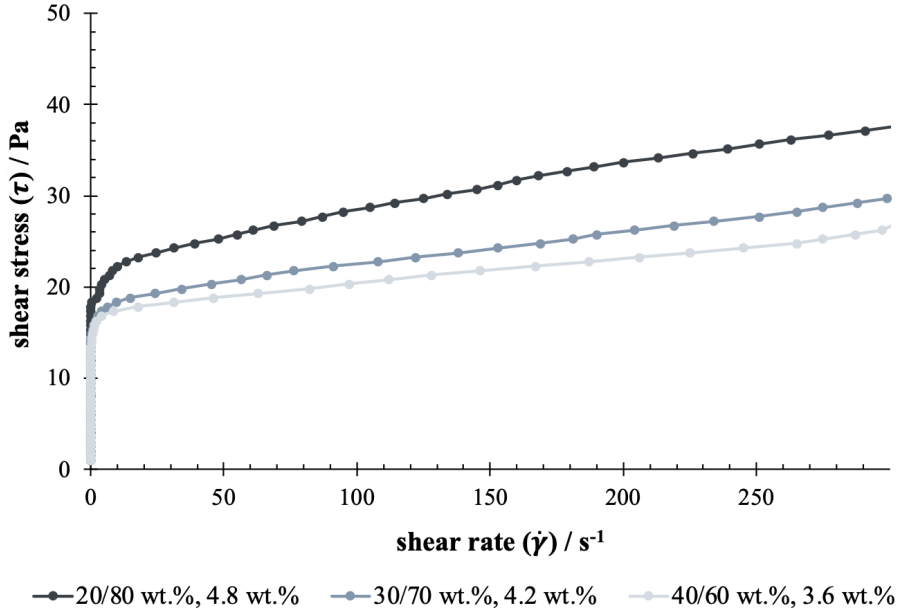

Figure 4.12. Flow curve of Pickering emulsions containing leek CMF at maximum PSC: shear stress (τ) versus shear rate ($\dot{\gamma}$).

Table 4.12. Rheological properties of Pickering emulsions containing leek CMF at maximum PSC: yield stress.

O/W ratio / wt.%	PSC / wt.%	Yield stress / Pa
20/80	4.8*	21
30/70	4.2*	18
40/60	3.6*	16

Figure 4.13 shows the amplitude sweep test, which is represented by the storage modulus (G') and loss modulus (G'') in function of the shear strain. G' represents the elastic portion of the viscoelastic behaviour, whereas G'' represents the viscous portion. For all emulsions, G' is always greater than G'' at low shear strains (γ). As shear strain increases, an intersection point between G' and G'' is observed. It corresponds to the shear strain at which deformation of emulsions occurs. The linear viscoelastic region (LVR) corresponds to the shear strain range before the interception of G' and G''. In LVR, the moduli of 20/80 wt.% O/W ratio at 4.8 wt.% PSC is higher, which relates once again to its higher stability.

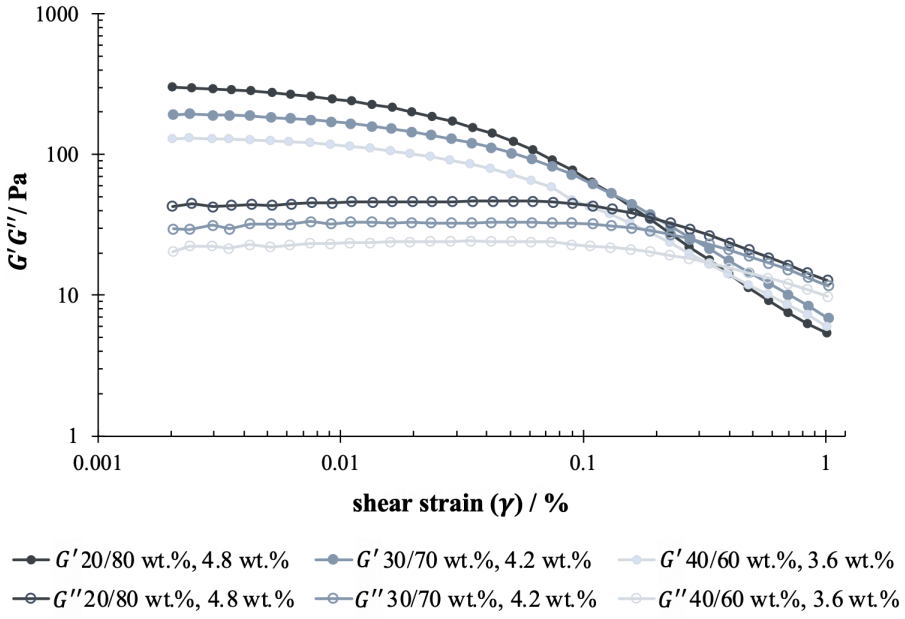

Figure 4.13. Amplitude sweep test for Pickering emulsions containing leek at maximum PSC: storage modulus (G') and loss modulus (G'') versus shear strain (γ).

At 0.01 % shear strain, all Pickering emulsions analysed are within LVR. Thus, shear strain was fixed at that value for the dynamic frequency sweep measurements. Figure 4.14 shows the frequency sweep test, where G' and G'' is a function of angular frequency (ω). Dynamic measurements are important to observe the emulsions' behaviour to an external deformation that is a periodic function of time within the non-destructive deformation range. High frequencies are used to simulate fast motion on short timescales, while low frequencies simulate slow motion on long timescales or at rest (Mezger, 2018).

As observed, both moduli are mostly independent of the frequency over the tested frequency range (40-100 rad s^{-1}). For 40/60 wt.% O/W ratio and 3.6 wt.% PSC, frequency dependence is observed for G''. In addition, G' is greater than G'', evidencing that the emulsions behaviour is predominantly elastic, i.e., solid-state dominant, which is consistent with the development of gel-like networks [1].

[1] Gels are solid-like materials with at least two components, one of which is a liquid, where $G > G''$. Ross-Murphy, S. B. (1994). Rheological characterization of polymer gels and networks. *Polymer Gels and Networks*, *2*, 229-237. https://doi.org/https://doi.org/10.1016/0966-7822(94)90007-8

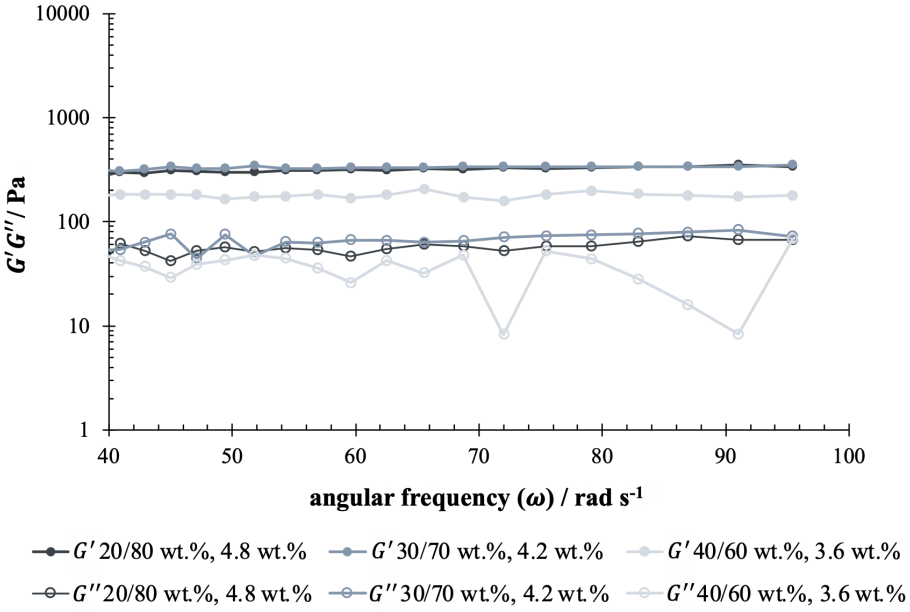

Figure 4.14. Rheological properties of leek Pickering emulsions at maximum PSC for different O/W ratios: storage modulus (G') and loss modulus (G'') versus angular frequency (ω).

5 Conclusion

In this work, leek and lettuce food waste were used as raw materials to mechanically obtain cellulose fibres that were used as stabilizers for oil-in-water Pickering emulsions. This approach ensures the full valorisation of the residues since it was unnecessary to extract the cellulose fraction from the pulps, which would have a low yield. The proposed alternative is of extreme relevance to prevent environmental damages and promote a circular economy.

Mechanical fibrillation was performed by a selection of pre-treatments – drying, milling, and disintegration in a blender with water – which proved to be the combination that enabled better fibre diameter reduction. Meanwhile, the drying of the raw materials enables longer conservation and easier transport.

Fibrillation was carried out by HPH at different consistencies (leek) and with and without centrifugation of the pre-treated pulp (lettuce). HPH was complemented with a morphological characterization that enabled fibrillation monitoring along the process. Lettuce showed higher fibrillation potential as concluded by the presence of smaller, more shredded fibres than leek's (OM images), which was confirmed by its higher aspect ratio and cationic demand, and lower polymerization degree. Furthermore, OM images showed a highly heterogeneous fibre size distribution, evidenced in the low transmittance values associated with the presence of fibres over the nano range.

Pickering emulsions, initially produced as proof of concept, successfully showed an emulsion phase after 48 h, proving the feasibility of using heterogeneous and over the nano range fibres produced from leek and lettuce residues as Pickering stabilizers. For each raw material, optimal stability was achieved at different fibrillation conditions, considering a fixed O/W ratio and PSC: for leek, with 6 passes of HPH at 600 bar and high consistency; for lettuce, with centrifugation of the pre-treated pulp and no HPH. Thus, as these results show, leek shows higher Pickering stabilization potential when fibres of nano and micro diameter are both present, whereas lettuce behaves oppositely. In both pulps, cellulose fibres were identified as CMF.

Finally, oil-in-water Pickering emulsions were produced with EI > 92 wt.% for O/W ratios of 20/80, 30/70, and 40/60 wt.%, generally the formulation at maximum PSC. It was observed that increasing PSC resulted in the increase of the emulsion phase, i.e., in higher EI.

CLSM showed the effective role of CMF as Pickering stabilizers. A mechanism of matrix stabilization was observed: the fibres of large diameters bend at the O/W interface and interconnect, forming a network that acts as the physical barrier against coalescence. It also showed oil droplets of heterogeneous sizes due to the broad fibre diameter distribution, causing the fibres to organize unevenly.

Therefore, the work described contributed as a positive proof of concept of using leek and lettuce food waste to produce pulps containing CMF that could act as Pickering emulsions stabilizers.

6 Assessment of the work done

6.1 Objectives Achieved

The objectives of this work were to obtain cellulose micro/nanofibres from leek and lettuce food waste and to produce stable Pickering emulsions formulations for future application in the food area. As described throughout this dissertation, heterogeneous cellulose fibres of nano and micro diameters were obtained for both raw materials after HPH mechanical treatment. When producing Pickering emulsions with lettuce, the absence of nanofibres was preferred. In the end, stable Pickering emulsions with EI higher than 92 wt.% were successfully stabilized using leek and lettuce pulps containing CMF.

6.2 Other Work Carried Out

In addition to leek and lettuce food waste, the same methodology of cellulose fibres production was performed on apple pomace, a by-product of cider production in Spain:

- adequate pre-treatments were selected by OM analysis;
- 9 passes of HPH were performed at high consistency. Compositional characterization was done, along with OM analysis and aspect ratio determination;
- preliminary tests were conducted to determine the fibre production conditions for Pickering emulsions application.

6.3 Limitations and Future Work

One of the main limitations of this dissertation was the lack of dried lettuce to produce more Pickering emulsions formulations and to characterize them through CLSM and rheological analyses.

Another difficulty was that the CMF was in pulp form, with a limiting consistency, which did not enable the production of emulsions with PSC above that value. Moreover, after 15 days, the pulps showed signs of fermentation even with the addition of biocide.

Finally, the OM analysis of the Pickering emulsions was highly challenging since the larger fibres covered the oil droplets. Therefore, stability after 48 h could only be measured by visual inspection.

In the future, other mechanical fibrillation techniques can be explored to obtain homogeneous CMF and compare the stability of their use as Pickering emulsions stabilizers with those presented in this dissertation. Additionally, cellulose can be isolated from the other components to study its effective role as Pickering stabilizer. Finally, the continuous production of Pickering emulsions, e.g., using NETmix technology, can be tested to scale up the production of the emulsions.

7 Bibliographic References

Albert, C., Beladjine, M., Tsapis, N., Fattal, E., Agnely, F., & Huang, N. (2019). Pickering emulsions: Preparation processes, key parameters governing their properties and potential for pharmaceutical applications. *Journal of Controlled Release*, *309*, 302-332. https://doi.org/10.1016/j.jconrel.2019.07.003

Araya-Chavarría, K., Rojas, R., Ramírez-Amador, K., Sulbarán-Rangel, B., Rojas, O., & Esquivel-Alfaro, M. (2022). Cellulose Nanofibers as Functional Biomaterial from Pineapple Stubbles via TEMPO Oxidation and Mechanical Process. *Waste and Biomass Valorization*, *13*, 1749-1758. https://doi.org/10.1007/s12649-021-01619-3

Balea, A. (2017). *Celulosa Nanofibrilada y su Aplicación en la Industria Papelera para la Mejora de Productos Reciclados* Universidad Complutense de Madrid].

Balea, A., Merayo, N., Fuente, E., Delgado-Aguilar, M., Mutje, P., Blanco, A., & Negro, C. (2016). Valorization of Corn Stalk by the Production of Cellulose Nanofibers to Improve Recycled Paper Properties. *BioResources*, *11*(2), 3416-3431. https://ojs.cnr.ncsu.edu/index.php/BioRes/article/view/BioRes_11_2_3416_Balea_Valorization_Corn_Stalk_Cellulose_Nanofibers

Binks, B. P., & Lumsdon, S. O. (2000). Influence of Particle Wettability on the Type and Stability of Surfactant-Free Emulsions. *Langmuir*, *6*, 8622-8631. https://doi.org/10.1021/la000189s

Blanco, A., Monte, M. C., Campano, C., Balea, A., Merayo, N., & Negro, C. (2018). Nanocellulose for Industrial Use. In *Handbook of Nanomaterials for Industrial Applications* (pp. 74-126). https://doi.org/10.1016/b978-0-12-813351-4.00005-5

Cadena, E. M., Garcia, J., Vidal, T., & Torres, A. L. (2009). Determination of zeta potential and cationic demand in ECF and TCF bleached pulp from eucalyptus and flax. Influence of measuring conditions. *Cellulose*, *16*, 491-500. https://doi.org/10.1007/s10570-009-9275-3

Chen, T., Colver, P. J., & Bon, S. A. F. (2007). Organic–Inorganic Hybrid Hollow Spheres Prepared from TiO2-Stabilized Pickering Emulsion Polymerization. *Advanced Materials*, *19*, 2286-2289. https://doi.org/10.1002/adma.200602447

Costa, A. L. R., Gomes, A., Tibolla, H., Menegalli, F. C., & Cunha, R. L. (2018). Cellulose nanofibers from banana peels as a Pickering emulsifier: High-energy emulsification processes. *Carbohydr Polym*, *194*, 122-131. https://doi.org/10.1016/j.carbpol.2018.04.001

Duan, L., Chen, M., Zhou, S., & Wu, L. (2009). Synthesis and Characterization of Poly(N-isopropylacrylamide)/Silica Composite Microspheres via Inverse Pickering Suspension Polymerization. *Langmuir*, *25*, 3467-3472. https://doi.org/10.1021/la8041617

Gonzalez Ortiz, D., Pochat-Bohatier, C., Cambedouzou, J., Bechelany, M., & Miele, P. (2020). Current Trends in Pickering Emulsions: Particle Morphology and Applications. *Engineering*, *6*, 468-482. https://doi.org/10.1016/j.eng.2019.08.017

Guillot, S., Bergaya, F., de Azevedo, C., Warmont, F., & Tranchant, J. F. (2009). Internally structured pickering emulsions stabilized by clay mineral particles. *Journal of Colloid and Interface Science*, *333*, 563-569. https://doi.org/10.1016/j.jcis.2009.01.026

He, K., Li, Q., Li, Y., Li, B., & Liu, S. (2020). Water-insoluble dietary fibers from bamboo shoot used as plant food particles for the stabilization of O/W Pickering emulsion. *Food Chem*, *310*, 125925. https://doi.org/10.1016/j.foodchem.2019.125925

ISO. (2017). Nanotechnologies - Standard terms and their definition for cellulose nanomateria. In (Vol. TS 20477).

Jimenez-Lopez, C., Fraga-Corral, M., Carpena, M., García-Oliveira, P., Echave, J., Pereira, A. G., Lourenço-Lopes, C., Prieto, M. A., & Simal-Gandara, J. (2020). Agriculture waste valorisation as a source of antioxidant phenolic compounds within a circular and sustainable bioeconomy. *Food & Function*(6). https://doi.org/10.1039/D0FO00937G

Li, X., Li, J., Kuang, Y., Guo, S., Mo, L., & Ni, Y. (2019). Stabilization of Pickering emulsions with cellulose nanofibers derived from oil palm fruit bunch. *Cellulose*, *27*(2), 839-851. https://doi.org/10.1007/s10570-019-02803-4

Lu, X., Zhang, H., Li, Y., & Huang, Q. (2018). Fabrication of milled cellulose particles-stabilized Pickering emulsions. *Food Hydrocolloids*, *77*, 427-435. https://doi.org/10.1016/j.foodhyd.2017.10.019

Lu, Z., Ye, F., Zhou, G., Gao, R., Qin, D., & Zhao, G. (2020). Micronized apple pomace as a novel emulsifier for food O/W Pickering emulsion. *Food Chem*, *330*, 127325. https://doi.org/10.1016/j.foodchem.2020.127325

Ma, Y., Luo, J., & Xu, Y. (2019). Co-preparation of pectin and cellulose from apple pomace by a sequential process. *J Food Sci Technol*, *56*(9), 4091-4100. https://doi.org/10.1007/s13197-019-03877-5

Marchand, V. (2010). Trans fats: What physicians should know. *Paediatr Child Health*, *15*(6), 373-375. https://doi.org/10.1093/pch/15.6.373

Mateo, S., Peinado, S., Morillas-Gutiérrez, F., La Rubia, M. D., & Moya, A. J. (2021). Nanocellulose from Agricultural Wastes: Products and Applications—A Review. *Processes*, *9*. https://doi.org/10.3390/pr9091594

Mezger, T. (2018). *Applied Rheology – With Joe Flow on Rheology Road* (A. P. GmbH, Ed. 2 ed.).

Nakatani, T., & Sato, S. (2017). Preparation of Nanofibrillated Cellulose in Powder Form. *Japan Tappi Journal*, *72*(2), 62-66. https://doi.org/https://doi.org/10.2524/jtappij.72.202

Nechyporchuk, O., Belgacem, M. N., & Bras, J. (2016). Production of cellulose nanofibrils: A review of recent advances. *Industrial Crops and Products*, *93*, 2-25. https://doi.org/10.1016/j.indcrop.2016.02.016

Negro, C., Balea, A., Sanchez-Salvador, J. L., Campano, C., Fuente, E., Monte, M. C., & Blanco, A. (2020). Nanocellulose and its Potential Use for Sustainable Industrial Applications. *Latin American Applied Research*, *50*(2). https://doi.org/10.52292/j.laar.2020.471

Pickering, S. U. (1907). CXCVI.—Emulsions. *J. Chem. Soc., Trans.*, *91*(0), 2001-2021. https://doi.org/10.1039/ct9079102001

Rao, P., & Rathod, V. (2018). Valorization of Food and Agricultural Waste: A Step towards Greener Future. *The Chemical Record*, *18*, 1-15. https://doi.org/10.1002/tcr.201800094

Rashid, S., & Dutta, H. (2020). Characterization of nanocellulose extracted from short, medium and long grain rice husks. *Industrial Crops and Products*, *154*. https://doi.org/10.1016/j.indcrop.2020.112627

Rhim, J.-W., Reddy, J. P., & Luo, X. (2015). Isolation of cellulose nanocrystals from onion skin and their utilization for the preparation of agar-based bio-nanocomposites films. *Cellulose*, *22*, 407-420. https://doi.org/10.1007/s10570-014-0517-7

Ribeiro, A., Manrique, Y. A., Barreiro, F., Lopes, J. C. B., & Dias, M. M. (2021). Continuous production of hydroxyapatite Pickering emulsions using a mesostructured reactor. *Colloids and Surfaces A: Physicochemical and Engineering Aspects*, *616*. https://doi.org/10.1016/j.colsurfa.2021.126365

Ribeiro, A., Manrique, Y. A., Ferreira, I. C. F. R., Barreiro, M. F., Lopes, J. C. B., & Dias, M. M. (2022). Nanohydroxyapatite (n-HAp) as a pickering stabilizer in oil-in-water (O/W) emulsions: a stability study. *Journal of Dispersion Science and Technology*, *43*(6), 814-826. https://doi.org/10.1080/01932691.2020.1845199

Rojas, J., Bedoya, M., & Ciro, Y. (2015). Current Trends in the Production of Cellulose Nanoparticles and Nanocomposites for Biomedical Applications. In *Cellulose - Fundamental Aspects and Current Trends*. https://doi.org/10.5772/61334

Ross-Murphy, S. B. (1994). Rheological characterization of polymer gels and networks. *Polymer Gels and Networks*, *2*, 229-237. https://doi.org/https://doi.org/10.1016/0966-7822(94)90007-8

Rotor-Stator Homogenization. Homogenizers. Retrieved 23 June 2022 from https://homogenizers.net/pages/ac-rotor-stator-homogenization

Sanchez-Salvador, J. L., Balea, A., Monte, M. C., Blanco, A., & Negro, C. (2019). Pickering Emulsions Containing Cellulose Microfibers Produced by Mechanical Treatments as Stabilizer in the Food Industry. *Applied Sciences*, *9*(2). https://doi.org/10.3390/app9020359

Sanchez-Salvador, J. L., Campano, C., Lopez-Exposito, P., Tarres, Q., Mutje, P., Delgado-Aguilar, M., Monte, M. C., & Blanco, A. (2021). Enhanced Morphological Characterization of Cellulose Nano/Microfibers through Image Skeleton Analysis. *Nanomaterials (Basel)*, *11*(8). https://doi.org/10.3390/nano11082077

Sun, Z., Yan, X., Xiao, Y., Hu, L., Eggersdorfer, M., Chen, D., Yang, Z., & Weitz, D. A. (2022). Pickering emulsions stabilized by colloidal surfactants: Role of solid particles. *Particuology*, *64*, 153-163. https://doi.org/10.1016/j.partic.2021.06.004

Tibolla, H., Pelissari, F. M., Martins, J. T., Lanzoni, E. M., Vicente, A. A., Menegalli, F. C., & Cunha, R. L. (2019). Banana starch nanocomposite with cellulose nanofibers isolated from banana peel by enzymatic treatment: In vitro cytotoxicity assessment. *Carbohydrate Polymers*, *207*, 169-179. https://doi.org/10.1016/j.carbpol.2018.11.079

Understand Yield Stress Measurements. (2015). Malvern Instruments. Retrieved 22 June 2022 from https://cdn.technologynetworks.com/TN/Resources/PDF/WP120416UnderstandYieldStressMeas.pdf

Varanasi, S., He, R., & Batchelor, W. (2013). Estimation of cellulose nanofibre aspect ratio from measurements of fibre suspension gel point. *Cellulose*, *20*, 1885-1896. https://doi.org/10.1007/s10570-013-9972-9

Zhang, G., Wu, F., Ma, T., Zhang, B., Manyande, A., & Du, H. (2019). Preparation and Characterization of Cellulose Nanofibers Isolated from Lettuce Peel. *Cellulose Chemistry and Technology*, *53*(7-8), 677-684. https://doi.org/10.35812/CelluloseChemTechnol.2019.53.66

Zuluaga, R., Putaux, J.-L., Restrepo, A., Mondragon, I., & Gañán, P. (2007). Cellulose microfibrils from banana farming residues: isolation and characterization. *Cellulose*, *14*(6), 585-592. https://doi.org/10.1007/s10570-007-9118-z

Appendix A - Particle size dependance on dispersion time and rotor-stator homogenizer speed

The influence of dispersion time and rotor-stator homogenizer speed during emulsification on leek CMF size distribution was studied. Four evaluations at different conditions, summarized in Table A.1, were performed using a laser diffraction particle size analyser (Beckman Coulter LS230, California, USA). Figure A.1 shows the obtained comparison of size distribution, in number.

Table A.1. Particle size dependence on dispersion time and rotor-stator homogenizer speed: conditions of the analysis.

Sample	Speed / rpm	Time of agitation / min
A	-	-
B	11 000	1
C	39 000	1
D	39 000	5

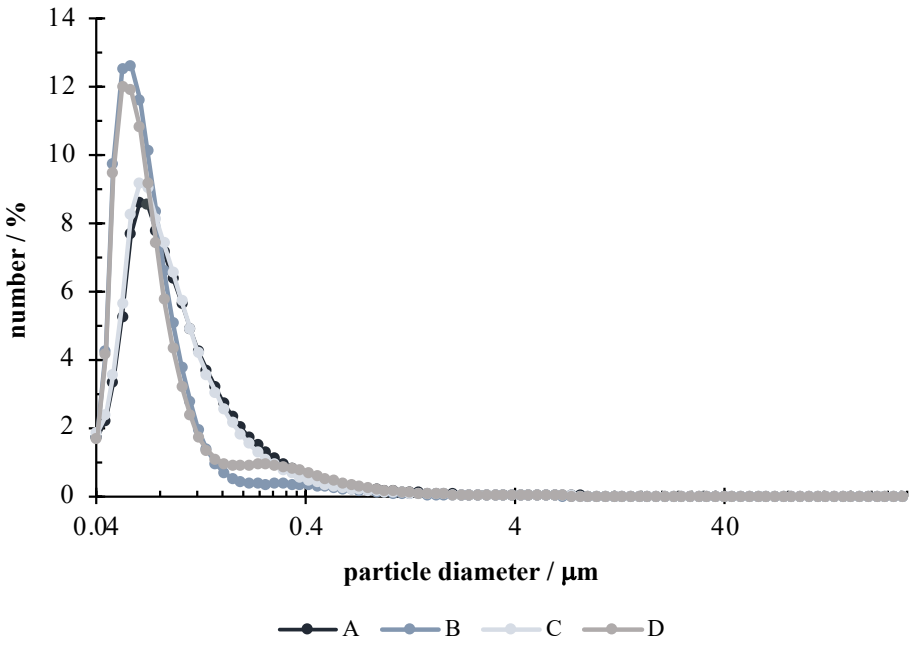

Figure A.1. Particle size dependence on dispersion time and rotor-stator homogenizer speed: (A) without agitation (0 rpm, 0 min); (B) 11 000 rpm, 1 min; (C) 39 000 rpm, 1 min; (D) 39 000 rpm, 5 min